AD-A093 106　ROME AIR DEVELOPMENT CENTER GRIFFISS AFB NY　F/G 20/6
STUDIES OF THE INTERACTIONS OF IONIZING RADIATIONS WITH COMMUNI--ETC(U)
NOV 80　M W WILLIAMS, J C ASHLEY
UNCLASSIFIED　RADC-TR-80-348　NL

1 of 1

END
DATE
FILMED
2-84
DTIC

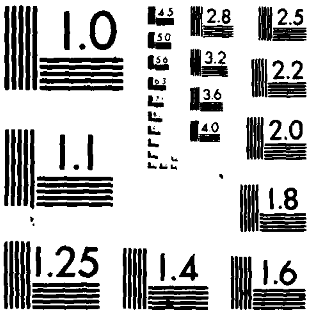

MICROCOPY RESOLUTION TEST CHART
NATIONAL BUREAU OF STANDARDS-1963-A

LEVEL II

(12)

RADC-TR-80-348
Interim Report
November 1980

STUDIES OF THE INTERACTIONS OF IONIZING RADIATIONS WITH COMMUNICATIONS MATERIALS

Oak Ridge National Laboratory

M.W. Williams
J.C. Ashley

ROME AIR DEVELOPMENT CENTER
Air Force Systems Command
Griffiss Air Force Base, New York 13441

This report has been reviewed by the RADC Public Affairs Office (PA) and is releasable to the National Technical Information Service (NTIS). At NTIS it will be releasable to the general public, including foreign nations.

RADC-TR-80-348 has been reviewed and is approved for publication.

APPROVED: John N Bradford

JOHN N. BRADFORD
Project Engineer

APPROVED: Clarence D. Turner

CLARENCE D. TURNER, Acting Director
Solid State Sciences Division

FOR THE COMMANDER: John P. Huss

JOHN P. HUSS
Acting Chief, Plans Office

If your address has changed or if you wish to be removed from the RADC mailing list, or if the addressee is no longer employed by your organization, please notify RADC (ESR), Hanscom AFB MA 01731. This will assist us in maintaining a current mailing list.

Do not return this copy. Retain or destroy.

(14) **REPORT DOCUMENTATION PAGE**

READ INSTRUCTIONS BEFORE COMPLETING FORM

1. REPORT NUMBER
RADC-TR-80-348

2. GOVT ACCESSION NO.
AD-A093 106

3. RECIPIENT'S CATALOG NUMBER
(9)

4. TITLE (and Subtitle)
(6) STUDIES OF THE INTERACTIONS OF IONIZING RADIATIONS WITH COMMUNICATIONS MATERIALS.

5. TYPE OF REPORT & PERIOD COVERED
Interim Report,
1 Oct 78-30 Sep 80,

6. PERFORMING ORG. REPORT NUMBER
N/A

7. AUTHOR(s)
(10) M.W./Williams
J.C./Ashley

8. CONTRACT OR GRANT NUMBER(s)
MIPR RADC 80-01

9. PERFORMING ORGANIZATION NAME AND ADDRESS
Oak Ridge National Laboratory
Health and Safety Research Division
Oak Ridge TN 37830

10. PROGRAM ELEMENT, PROJECT, TASK AREA & WORK UNIT NUMBERS
61102F
(16) 2306J320 (17) J3

11. CONTROLLING OFFICE NAME AND ADDRESS
Deputy for Electronic Technology (RADC/ESR) (11)
Hanscom AFB MA 01731

12. REPORT DATE
Nov[redacted]80

13. NUMBER OF PAGES
66 (12) 62

14. MONITORING AGENCY NAME & ADDRESS (if different from Controlling Office)
Same

15. SECURITY CLASS. (of this report)
UNCLASSIFIED

15a. DECLASSIFICATION/DOWNGRADING SCHEDULE
N/A

16. DISTRIBUTION STATEMENT (of this Report)

Approved for public release; distribution unlimited

17. DISTRIBUTION STATEMENT (of the abstract entered in Block 20, if different from Report)

Same

18. SUPPLEMENTARY NOTES

RADC Project Engineer: John N. Bradford (ESR)

19. KEY WORDS (Continue on reverse side if necessary and identify by block number)

Optical properties of Kapton
Electron
Mean free path
Nuclear reaction-proton

20. ABSTRACT (Continue on reverse side if necessary and identify by block number)

This report summarizes experimental and theoretical studies designed to yield information on the interaction of ionizing radiations with various communications materials. The optical properties of Kapton have been measured over the energy range from 0.5 eV to 76 eV. Theoretical models combined with experimental optical data have been used to calculate mean excitation energies, mean free paths, and stopping powers for low-energy electrons (100 eV to 10 keV) in various solid organic insulators. (over)

(cont)

The contribution to both the mean free path and stopping power due to K-shell ionizations in carbon, nitrogen, and oxygen where then obtained from theoretical atomic generalized oscillator strengths and added to the valence electron contributions. A model involving the diffusion of excitons has been proposed to explain data, reported in the literature, showing that a thin metallic surface layer may partially protect organic crystals against radiation damage. The stopping powers of several metals for electrons have been calculated from an electron gas statistical model and used to calculate the continuous slowing-down-approximation range and range straggling for electrons with energies $\leq$ 10 keV. Microdosimetric calculations have been made of the structure of heavy-ion tracks in silicon. Results show that these tracks are very small in lateral extent compared with the dimensions of critical volumes in currently used microelectronic components. In addition, calculations have been made of the spectrum of heavy particles which results when an energetic proton collides with a silicon nucleus.

< or =

CONTENTS

PROGRAM SUMMARY 4

I. MEASUREMENT OF OPTICAL PROPERTIES 6

- A. Polyethylene 6
- B. Kapton 6

II. DETERMINATION OF ELECTRON TRANSPORT PARAMETERS 7

- A. Mean Excitation Energies, Mean Free Paths, and Stopping Powers 7
- B. Ranges of Low-Energy Electrons in Solids 7

III. "UNIVERSAL" CURVES 9

- A. Electron Mean Free Paths 9
- B. Stopping Powers for Electrons 14

IV. PROTECTION AGAINST RADIATION DAMAGE TO ORGANIC CRYSTALS: EXCITON EFFECTS 15

V. MICRODOSIMETRY 16

- A. Heavy-Ion Track Structure in Silicon 16
- B. Proton-Induced Recoil Spectra in Silicon 17

PUBLICATIONS AND PRESENTATIONS 21

APPENDIX A. THE OPTICAL PROPERTIES OF KAPTON: MEASUREMENT AND APPLICATIONS.

APPENDIX B. INELASTIC INTERACTIONS OF LOW-ENERGY ELECTRONS WITH ORGANIC SOLIDS: SIMPLE FORMULAE FOR MEAN FREE PATHS AND STOPPING POWERS.

PROGRAM SUMMARY

This report summarizes work done in an ongoing program under contract RAD 80007 for the periods October 1978 through September 1979 (Project Order RADC 79-04) and October 1979 through September 1980 (Project Order RADC 80-01). The objective is to gain information on the interaction of ionizing radiations with various communications materials. Thus, the intent is that work performed under this contract will increase our understanding of the basic mechanisms involved when photons, electrons, or other ionizing radiations interact with matter in its condensed phases. Emphasis is being placed on studying the interactions occurring in those materials which are currently used, or which are being considered for use, in electronics systems. Knowledge of quantities such as the cross sections for the various types of electron interactions in these materials enables predictions to be made concerning the performance of electronics systems in various situations, such as exposure to the results of a nuclear explosion. Our approach to this general problem is both theoretical and experimental. In our experimental program, we continue to make observations which can be related to photon and electron interactions with solids. The theoretical portions of the program include predictive calculations for a variety of interaction phenomena as well as interpretative studies in support of our experimental efforts. Results from the basic theoretical and experimental programs are employed in applied calculations with direct relevance to the performance of electronics systems including microsystems produced by VLSI technology.

During this 2-year period we have largely concentrated on organic materials. Optical properties have been measured and the values obtained have been used in the calculation of transport parameters for ionizing radiations incident on the selected organic materials. Our studies have led us to propose "universal" relations for the mean free paths and stopping powers for electrons in solid organic insulators. We have also considered, theoretically, possible mechanisms associated with the protection of organic crystals against radiation damage. Work has continued in the field of microdosimetry with the calculation of both heavy-ion track structure and proton-induced recoil spectra in silicon.

The material described in this report is the result of the collaborative efforts of the following scientists:

(1) E. T. Arakawa, J. C. Ashley, R. N. Hamm, R. H. Ritchie, J. E. Turner, M. W. Williams, and H. A. Wright, Health and Safety Research Division, and V. E. Anderson, Computer Sciences Division, ORNL.

(2) C. J. Tung, Institute of Nuclear Science, National Tsing Hua University, Hsinchu, Taiwan 300, Republic of China.

(3) Martin Pope, Department of Chemistry, New York University, New York, New York 10003.

(4) T. A. Callcott and L. R. Painter, Department of Physics and Astronomy, University of Tennessee, Knoxville, Tennessee 37916.

(5) M. L. Rustgi, on sabbatical leave from the Department of Physics, State University of New York at Buffalo, Amherst, New York 14260.

Finally, we gratefully acknowledge the continuing advice and support of J. N. Bradford of the Rome Air Development Center.

I. MEASUREMENT OF OPTICAL PROPERTIES

A knowledge of the optical properties of a material over an energy range which covers essentially all of the oscillator strength associated with the valence electrons enables us to calculate the transport parameters associated with the interaction of ionizing radiations with that material. Thus, for a number of years we have been measuring the optical properties of materials over an extended energy range. Over the past few years we have concentrated on organic materials in a condensed phase. Work in this reporting period has involved two materials:

A. Polyethylene

Work started in the previous reporting period (see report RADC-TR-79-234) was completed and published [L. R. Painter, E. T. Arakawa, M. W. Williams, and J. C. Ashley, *Radiat. Res.* 83, 1-18 (1980)].

B. Kapton

Measurements were initiated and completed for Kapton. A preprint of the results from this work, as submitted to the *Journal of Applied Physics*, forms Appendix A of this report.

II. DETERMINATION OF ELECTRON TRANSPORT PARAMETERS

A. Mean Excitation Energies, Mean Free Paths, and Stopping Powers

The measured optical data for a material may be used to calculate various electron transport parameters for that material. One such parameter is the mean excitation energy I, an important constant in the Bethe theory of stopping power. Values of I for polystyrene and polyethylene were calculated from the optical data for these solids. We found the values I = 68.7 eV for polystyrene [J. C. Ashley, *Phys. Rev. B* 19, 5429-5430 (1979)] and I = 62 eV for polyethylene [L. R. Painter, E. T. Arakawa, M. W. Williams, and J. C. Ashley, *Radiat. Res.* 83, 1-18 (1980)]. Other parameters which can be calculated from a knowledge of the optical constants over an extended energy range are the mean free path and the energy loss per unit pathlength, or stopping power, for electrons in the material. A model insulator theory, with parameters fixed by the optical data, was employed to calculate inverse mean free paths and stopping powers for low-energy electrons (10 eV through 10 keV) in polyethylene [L. R. Painter et al., *Radiat. Res.* 83, 1-18 (1980)]. Another theoretical model involving a fit to the energy-loss function calculated from the optical data was used to estimate electron mean free paths and stopping powers for low-energy electrons in Kapton (see Appendix A).

B. Ranges of Low-Energy Electrons in Solids

The stopping powers of Al, Au, Ag, and Cu for electrons were calculated from an electron gas statistical model including corrections to the stopping power due to the Z_1^3 effect. From these stopping powers the continuous-slowing-down-approximation (CSDA) range and range straggling were determined for electrons with energies ≤ 10 keV. Comparisons of the calculated CSDA ranges with experimental data were made. This work was published in the following reference: C. J. Tung, J. C. Ashley, and R. H. Ritchie, *IEEE Trans. Nucl. Sci.* NS-26, 4874-4878 (1979).

III. "UNIVERSAL" CURVES

A concerted effort is being made to determine "universal" relations by which transport parameters, such as electron mean free path, can be calculated for any material as a function of electron energy. During this reporting period we have established universal relations for the mean free path and stopping power of low-energy electrons (100 eV to 10 keV) in solid organic insulators.

A. Electron Mean Free Paths

A simple expression involving the molecular weight and density of an organic sample has been found for calculating the mean free path, Λ, for electrons in solid organic insulators in the energy range 100 eV to 10 keV. The expression is based on a theoretical formula for Λ with input parameters derived from the experimental optical spectra for solid organic insulators which were available over a sufficiently large energy range. These data consisted of the optical properties of DNA, bovine plasma albumin, adenine, guanine, polyethylene, and polystyrene, all of which had been obtained in our laboratory over the past few years. As the optical properties of Kapton (Appendix A) became available, it became possible to check our universal curve. These procedures and results are outlined in the following submission to the Proceedings of the VIth International Conference on Vacuum Ultraviolet Radiation Physics, University of Virginia, Charlottesville, Virginia, June 2-6, 1980, Vol. I-67, pp. 1-3.

ELECTRON MEAN FREE PATHS IN SOLID ORGANIC INSULATORS*

M. W. Williams and J. C. Ashley

Health and Safety Research Division
Oak Ridge National Laboratory
Oak Ridge, Tennessee 37830

The concept of electron mean free path, Λ, is integral to calculations of transport phenomena in condensed media. In the case of biological molecules this parameter is difficult to measure accurately, so we have formulated an empirical relation from which the mean free path of an electron in any solid organic insulator can be calculated over the range of electron energies from 100 eV to 10 keV.

The mean free path of electrons in a medium can be calculated from the optical properties for that medium over the whole frequency range.[1] We calculated Λ as a function of electron energy E from 100 eV to 10 keV for each of the six organic insulators (DNA, bovine plasma albumin, adenine, guanine, polyethylene, and polystyrene) for which the optical properties over essentially all of the oscillator strength of the valence electrons were available. For each material the relation between Λ and E was found to be of the form

$$\Lambda(E) = E/[A\,\ln E + B - C/E] ,$$

where the constants A, B, and C depend on the material. To represent the mean free paths for all solid organic insulators by a common formula, the assumption was then made that A, B, and C are each functions of n_v, the valence electron density. Analysis then showed that $A \propto n_v$, $B \propto n_v$, and $C \propto n_v$. Putting our results in terms of $\xi = \rho n/M$, where ρ is the density of the material in $g \cdot cm^{-3}$, n is the number of valence electrons per molecule or monomeric unit, and M is the molecular weight of the molecule or monomeric

---

[*] Research sponsored jointly by the Deputy for Electronic Technology, Air Force Systems Command, under Interagency Agreement DOE No. 40-226-70 and the Office of Health and Environmental Research, U.S. Department of Energy, under contract W-7405-eng-26 with the Union Carbide Corporation.

unit in g·mol^{-1}, we obtained[1] the equation

$$\Lambda\xi = E/[13.5\ \ln E - 20.9 - 821/E] , \qquad (1)$$

which was predicted to relate Λ in angstroms to E in electron volts for any solid organic insulator for which ρ, n, and M are known.

The calculations described in Ref. 1 have been repeated with a restriction on the allowable values of energy transfer to account, in an approximate fashion, for the effects of exchange between the incident electron and the valence electrons in the solid. In addition, an increase in the effective number of valence electrons by a factor of 1.05 due to oscillator strength coupling between core and valence electrons has now been incorporated in the expression for Λ. With these changes, but still neglecting the small contributions from inner-shell ionization,[1] the mean free path may now be written

$$\Lambda\xi = E/[13.6\ \ln E - 17.6 - 1400/E] . \qquad (2)$$

A plot of $\Lambda\xi$ versus E, as given by Eq. 2 is shown in Fig. 1. Mean free paths calculated from Eq. 2 are $<5\%$ smaller than those predicted by Eq. 1 for $E \gtrsim 200$ eV, equal at 150 eV, and ~6% larger at 100 eV. Shown on either side of this curve are the plots obtained directly from the optical properties for the individual materials, bovine plasma albumin and polystyrene, which were found to have the largest deviations from the average curve. Based on these data, the universal curve given by Eq. 2 is expected to predict values of mean free path to better than ±10% for all organic insulators over the energy range from 100 eV to 10 keV.

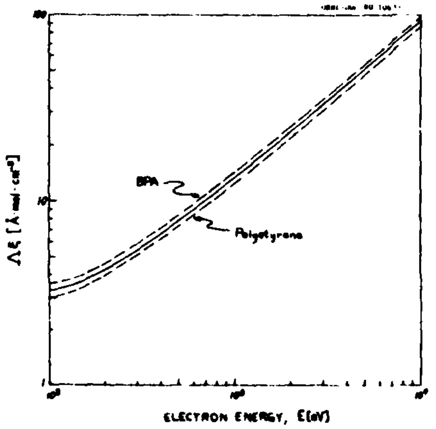

Fig. 1. The plot of $\Lambda\xi$ versus E as given by Eq. 2 plus the plots for bovine plasma albumin and polystyrene obtained directly from the optical properties.

The optical properties of Kapton Type H polyimide film have been measured recently in our laboratory, over essentially all of the oscillator strength of the valence electrons.[2] Figure 2 shows the values of Λ from 100 eV to 10 keV calculated from these optical data and as predicted from Eq. 2. It is seen that there is excellent agreement. The difference between the two curves ranges from 5% at 100 eV to <3% at 10 keV. This is well within the accuracy claimed for the universal mean-free-path relation given by Eq. 2.

It is anticipated that Eq. 2 should also predict the mean free paths of electrons in liquid organic insulators, including water. Confirmation must await the availability of optical data to higher energies.

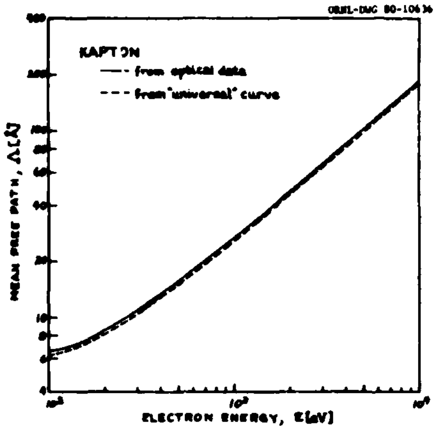

Fig. 2. Comparison of the mean free path of Kapton calculated as a function of electron energy from the optical data and from the universal relation given by Eq. 2.

References

1. J. C. Ashley and M. W. Williams, "Electron Mean Free Paths in Solid Organic Insulators," *Rad. Res.* 81, 364-373 (1980).
2. E. T. Arakawa, M. W. Williams, J. C. Ashley, and L. R. Painter, "The Optical Properties of Kapton: Measurement and Applications" (to be published).

As mentioned at the end of the previous preprint, we anticipated that this approach should work for water. Although experimental optical data for water are not available over an energy range that covers all the oscillator strength of the valence electrons, an estimated spectrum exists (R. H. Ritchie, R. N. Hamm, J. E. Turner, and H. A. Wright, "The Interaction of Swift Electrons with Liquid Water," VIth Symposium on Microdosimetry, Eds. J. Booz and H. G. Ebert, Brussels, Belgium, May 22-26, 1978, Vol. I, pp. 345-354). Shown in the figure below is the dependence of Λ on E for electrons in water derived from the universal equation for Λ and from the estimated optical spectrum for water. It is seen that there is excellent agreement.

ORNL-DWG 80-12698

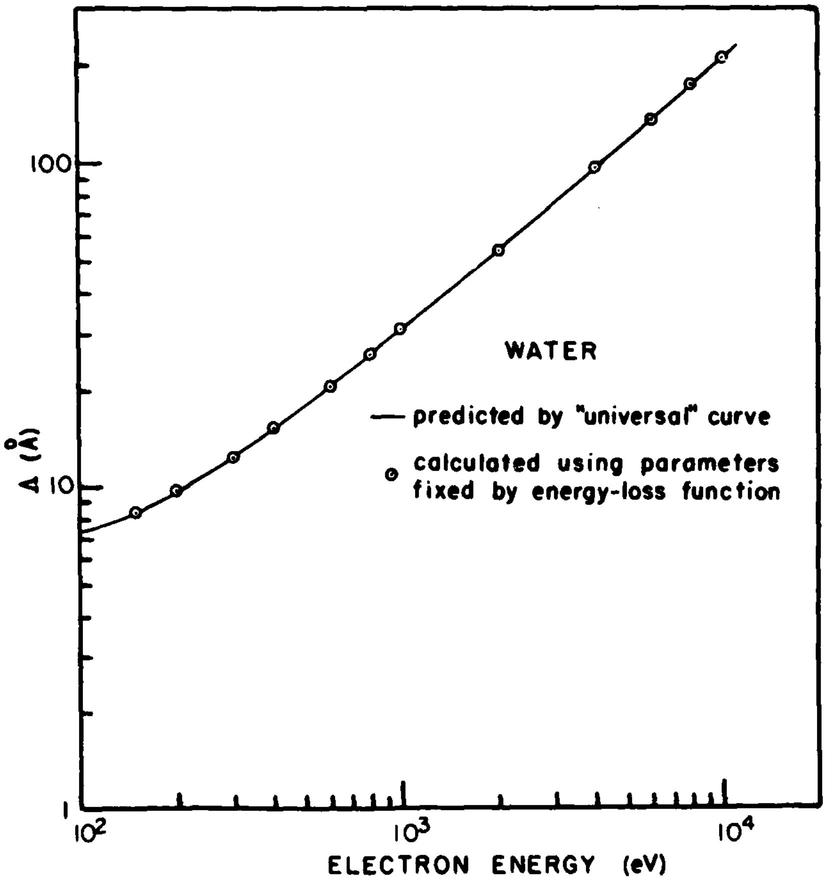

B. Stopping Powers for Electrons

A procedure similar to that described in part A has been used to obtain a universal relation for the stopping power for low-energy electrons due to the valence electrons in organic solids. The contributions to both the mean free path and the stopping power due to K-shell ionization in carbon, nitrogen, and oxygen were then obtained from theoretical atomic generalized oscillator strengths and added to the valence electron contributions. This work is described in the preprint forming Appendix B. This paper has been accepted for publication in the *IEEE Transactions on Nuclear Science.*

IV. PROTECTION AGAINST RADIATION DAMAGE TO ORGANIC CRYSTALS: EXCITON EFFECTS

Experimental measurements by Salih and Cosslett [*Philos. Mag.* 30, 225 (1974)] indicate that radiation damage to organic crystals of anthracene and coronene may be reduced by factors of 3 to 5 by coating the crystals with thin layers (50-100 Å) of aluminum or gold. They suggested that these results might be explained by neutralization of ions or holes in the crystal by electrons that tunnel from the metal overcoating.

An alternative mechanism to explain these observations has been proposed, i.e., that excitons, that would give rise to lattice defects in the absence of the overcoating layers, are quenched at the metal-crystal interface. Quantitative estimates based on an exciton diffusion model indicate that this alternative mechanism may be important in the Salih-Cosslett experiments. Details of, and predictions from, this model have been published. See: R. H. Ritchie and Martin Pope, *Philos. Mag. B* 40, 503-506 (1979).

V. MICRODOSIMETRY

The history of the development of electronics components has been one of continuous reduction in size, and this trend is expected to continue for some time. In present day large-scale integrated circuit technology, critical volumes, such as the active region in a memory chip, have been reduced to dimensions of the order of 10 μm. This is in the size domain which has been of interest in the field of microdosimetry in connection with radiation dose deposition of significance for biological effects. Microdosimetric calculations are now being applied to help in the understanding of radiation effects in solid-state electronics components.

In the past few years the phenomenon of cosmic-ray-induced "soft errors" in satellite computer memories has been observed. This is attributed to heavy charged particles producing sufficient ionization within a critical volume to change the bit stored in that location. We have undertaken two investigations in this field. In one we have used a Monte Carlo transport code to calculate the radial dependence of dose deposited in the vicinity of a heavy-ion track in silicon. This was undertaken to investigate the validity of error induction models in which it is assumed that a track may be treated as a line along which energy is deposited. In the other we have calculated the spectrum of heavy-recoil particles which result when an energetic proton collides with a silicon nucleus.

A. Heavy-Ion Track Structure in Silicon

The energy deposition in the vicinity of a heavy-ion path in silicon was investigated by a Monte Carlo transport analysis of the delta rays produced along the track. The dose as a function of radial distance was calculated for C, Al, and Fe ions with energies between 10 and 10^4 MeV. The average dose deposited in a cylinder, parallel to the track and having a radius between 10^{-3} and 1 μm, as a function of the distance of the axis of the cylinder from the path was also determined.

The results show that an ion track is very small in lateral extent as compared with the sizes of critical regions in present day semiconductor memory cells (∿10 μm). This remains true even for a reduction in the dimensions of the critical region by an order of magnitude. It is therefore expected that a model in which ion tracks are treated as mathematical lines along which energy is deposited in accordance with the stopping power should be valid. The publication describing these calculations and results is: R. N. Hamm, J. E. Turner, H. A. Wright, and R. H. Ritchie, *IEEE Trans. Nucl. Sci.* NS-26, 4892-4895 (1979).

B. Proton-Induced Recoil Spectra in Silicon

Protons ionize too sparsely to deposit enough charge within the critical volumes of present semiconductor memory chips to produce soft errors. However, protons may undergo nuclear interactions with the nuclei in the semiconductor material and produce heavy recoils which are capable of depositing a sufficient concentration of charge. We have used a nuclear interaction model to calculate the recoil spectra of heavy fragments produced when protons are incident on silicon.

The calculations were performed using MECC-7, Medium-Energy Intranuclear Cascade Code System. This code was developed at Oak Ridge National Laboratory and is available from the Radiation Shielding Information Center at Oak Ridge.

In this code an incoming nucleon distributes its energy among its collision partners, the nucleons, inside the target nucleus until it escapes from the nucleus or until it loses most of its kinetic energy and at last is captured in the nuclear potential. The evaporation process which follows the intranuclear cascade makes use of the work of Le Couteur [*Proc. Phys. Soc.* (London) 63A, 259 (1950)]. Use is made of free particle nucleon-nucleon data whenever cross-section data are needed. These data as well as the nuclear target configurations are specified on a tape used by MECC-7. The point of collision, the type of collision, the momentum of the struck nucleon, and the scattering angles, etc., are determined by statistical sampling techniques. The incident particles may be protons or neutrons with energies up to about 2500 MeV. The option exists for producing at least one pion where one pion production is energetically feasible.

Calculations were made for protons with energies of 20, 100, 130, 200, and 400 MeV incident on ^{28}Si. For each of these incident proton energies, we obtained the cross sections for production of various residual nuclei as well as for the particles directly produced by the cascade and evaporation: p, n, d, t, ^{3}He, and α. For each of these particles and residual nuclei, we obtained a production energy spectrum.

The calculations for 130 MeV incident protons were compared with the results of McNulty et al. (P. J. McNulty, G. E. Farrell, R. C. Wyatt, P. L. Rothwell, R. C. Filz, and J. N. Bradford, to be published in *IEEE Transactions on Nuclear Science*). Though the fragment mass spectra are very similar, two differences were observed. In our calculation the mass spectrum peaked at the mass number A=27, while in McNulty et al.'s calculation it peaked at A=25. Secondly, in our calculation, no fragments with $5 \leq A \leq 9$ were observed. In the following figure we compare our calculated recoil energy spectra with their measurement of energy deposition in a silicon slab of 24.1-μm thickness. The line labeled $10 \leq A \leq 28$ is our calculated absolute cross section for production of recoils in the indicated mass interval having energy greater than E as a function of E. The straight-line fit to their experimental data is normalized to our calculation at 2 MeV. The other line is our calculated results when the evaporated particles, p, d, t, ^{3}He and α, are included. It is also

ORNL DWG 80-18397R

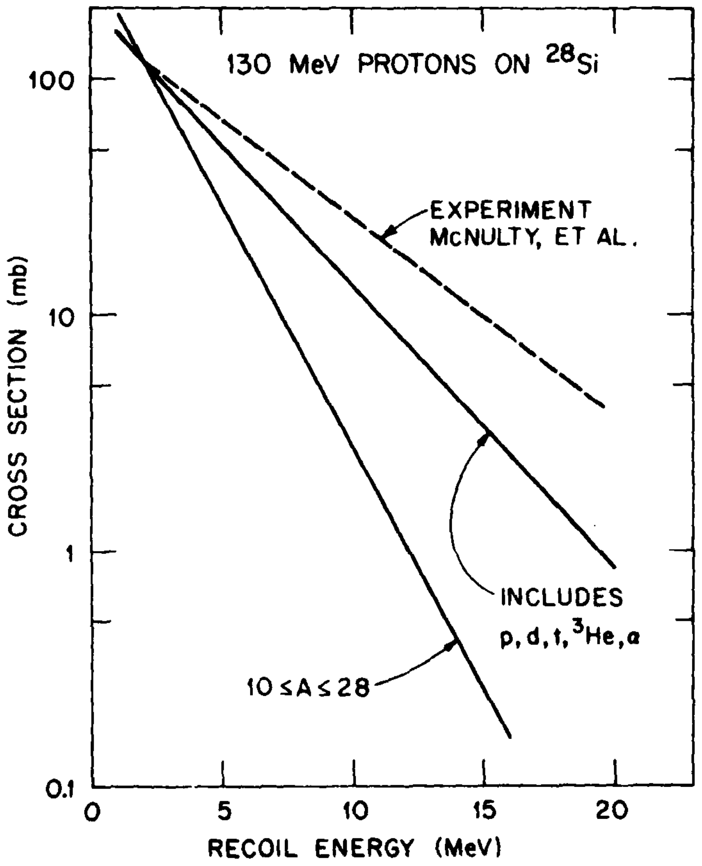

normalized to the other curves at 2 MeV. We find an exponential dependence of cross section on recoil energy in agreement with experiment, but our cross section falls off much more rapidly with increasing energy, and thus we would predict relatively fewer high-energy recoils. The calculated cross section for ^{28}Si recoil with energy greater than E was also plotted but could not be compared with observations for lack of data.

The lack of agreement could be attributed to the exclusion of several important processes not considered in the code. Among the processes which become important at higher energies is the spallation process in which the target nucleus is spalled into several pieces by the bombardment of energetic protons. Such fragmentation has recently been seen when target nuclei are bombarded with α particles, ^{12}C, ^{16}O, and other heavier projectiles. The energy spectra and angular distributions of these fragments differ from standard compound-nucleus theory expectations. The present code also does not take into account the knockout of certain light nuclei, such as α particles. This process of course becomes important at higher energies while the compound nucleus model works well at lower energies.

PUBLICATIONS AND PRESENTATIONS

During this reporting period several papers were published, or prepared for publication, and presentations were given at conferences which describe work related to this project and for which partial support by the Air Force was acknowledged. A list of these items follows.

Publications

J. C. Ashley, C. J. Tung, and R. H. Ritchie, "*Inelastic Interactions of Electrons with Polystyrene: Calculations of Mean Free Paths, Stopping Powers, and CSDA Ranges,*" IEEE Trans. Nucl. Sci. NS-25, 1566-1570 (1978).

E. Kretschmann, T. L. Ferrell, and J. C. Ashley, "*A Splitting of the Dispersion Relation of Surface Plasmons on a Rough Surface,*" Phys. Rev. Lett. 42, 1312-1314 (1979).

J. C. Ashley, V. E. Anderson, J. J. Cowan, R. H. Ritchie, and J. Hoelzl, "*Straggling and Plasmon Excitation in the Energy Loss Spectra of Electrons Transmitted through Carbon,*" Thin Solid Films 60, 361-370 (1979).

J. C. Ashley, "*Mean Excitation Energy of Polystyrene,*" Phys. Rev. B 19, 5429-5430 (1979).

T. L. Haltom, E. T. Arakawa, M. W. Williams, and E. Kretschmann, "*Refractive Index of LiF Films as a Function of Time,*" Appl. Opt. 18, 1233-1236 (1979).

J. C. Ashley, C. J. Tung, and R. H. Ritchie, "*Electron Inelastic Mean Free Paths and Energy Losses in Solids: I. Aluminum Metal,*" Surf. Sci. 81, 409-426 (1979).

C. J. Tung, J. C. Ashley, and R. H. Ritchie, "*Electron Inelastic Mean Free Paths and Energy Losses in Solids: II. Electron Gas Statistical Model,*" Surf. Sci. 81, 427-439 (1979).

M. W. Williams, J. C. Ashley, E. Kretschmann, T. A. Callcott, M. S. Chung, and E. T. Arakawa, "*Splitting of Surface Plasmon Emission Spectra from Potassium,*" Phys. Lett. 73A, 231-233 (1979).

R. H. Ritchie and Martin Pope, "*Protection Against Radiation Damage to Organic Crystals: Exciton Effects,*" Philos. Mag. B 40, 503-506 (1979).

R. N. Hamm, J. E. Turner, H. A. Wright, and R. H. Ritchie, "*Heavy-Ion Track Structure in Silicon,*" IEEE Trans. Nucl. Sci. NS-26, 4892-4895 (1979).

C. J. Tung, J. C. Ashley, and R. H. Ritchie, "*Range of Low-Energy Electrons in Solids,*" IEEE Trans. Nucl. Sci. NS-26, 4874-4878 (1979).

M. S. Chung, T. A. Callcott, E. Kretschmann, and E. T. Arakawa, *"Radiation from Silver Films Bombarded by Low-Energy Electrons,"* Surf. Sci. 91, 245-263 (1980).

E. Kretschmann, T. A. Callcott, and E. T. Arakawa, *"Theory of Emission Spectra from Metal Films Irradiated by Low-Energy Electrons Near Normal Incidence,"* Surf. Sci. 91, 237-244 (1980).

J. C. Ashley and M. W. Williams, *"Electron Mean Free Paths in Solid Organic Insulators,"* Radiat. Res. 80, 364-373 (1980).

L. R. Painter, E. T. Arakawa, M. W. Williams, and J. C. Ashley, *"Optical Properties of Polyethylene: Measurement and Applications,"* Radiat. Res. 83, 1-18 (1980).

L. R. Painter, E. T. Arakawa, M. W. Williams, and J. C. Ashley, *"The Optical Properties of Kapton: Measurement and Applications,"* Proceedings of the Topical Conference on Basic Optical Properties of Materials, National Bureau of Standards, Gaithersburg, Maryland, May 5-7, 1980, NBS Special Publication 574, pp. 20-23.

M. W. Williams and J. C. Ashley, *"Electron Mean Free Paths in Solid Organic Insulators,"* Proceedings of the VIth International Conference on Vacuum Ultraviolet Radiation Physics, University of Virginia, Charlottesville, Virginia, June 2-6, 1980, Vol. I-67 (3 pages).

J. C. Ashley, *"Inelastic Interactions of Low-Energy Electrons with Organic Solids: Simple Formulae for Mean Free Paths and Stopping Powers,"* IEEE Transactions on Nuclear Science (to be published).

E. T. Arakawa, M. W. Williams, J. C. Ashley, and L. R. Painter, *"The Optical Properties of Kapton: Measurement and Applications,"* Journal of Applied Physics (to be published).

R. N. Hamm, J. E. Turner, H. A. Wright, and R. H. Ritchie, *"Calculated Distance Distributions of Energy Transfer Events in Irradiated Liquid Water,"* Proceedings of the Seventh Symposium on Microdosimetry, Oxford, UK, September 8-12, 1980 (to be published).

H. A. Wright, R. N. Hamm, and J. E. Turner, *"Interface Effects on Dose Distributions in Irradiated Media,"* Proceedings of the Seventh Symposium on Microdosimetry, Oxford, UK, September 8-12, 1980 (to be published).

Previous final technical reports in this series are:

RADC-TR-77-74	(February 1977),AD040907
RADC-TR-79-234	(October 1979),AD079054

Presentations

C. J. Tung, J. C. Ashley, and R. H. Ritchie, *"Range of Low-Energy Electrons in Solids,"* IEEE Annual Conference on Nuclear and Space Radiation Effects, Santa Cruz, California, July 17-20, 1979.

R. N. Hamm, J. E. Turner, H. A. Wright, and R. H. Ritchie, *"Heavy Ion Track Structure in Silicon,"* IEEE Annual Conference on Nuclear and Space Radiation Effects, Santa Cruz, California, July 17-20, 1979.

M. W. Williams and J. C. Ashley, *"Electron Mean Free Paths in Solid Organic Insulators,"* Sixth International Conference on Vacuum Ultraviolet Radiation Physics, University of Virginia, Charlottesville, Virginia, June 2-6, 1980.

L. R. Painter, E. T. Arakawa, M. W. Williams, and J. C. Ashley, *"The Optical Properties of Kapton: Measurement and Applications,"* Topical Conference on Basic Optical Properties of Materials, National Bureau of Standards, Gaithersburg, Maryland, May 5-7, 1980.

J. C. Ashley, *"Stopping Powers of Organic Solids for Low-Energy Electrons,"* Radiation Research Society Annual Scientific Meeting, New Orleans, Louisiana, June 1-5, 1980.

J. C. Ashley, *"Inelastic Interactions of Low-Energy Electrons with Organic Solids: Simple Formulae for Mean Free Paths and Stopping Powers,"* IEEE Annual Conference on Nuclear and Space Radiation Effects, Cornell University, Ithaca, New York, July 15-18, 1980.

R. N. Hamm, J. E. Turner, H. A. Wright, and R. H. Ritchie, *"Calculated Distance Distributions of Energy Transfer Events in Irradiated Liquid Water,"* Seventh Symposium on Microdosimetry, Oxford, UK, September 8-12, 1980.

H. A. Wright, R. N. Hamm, and J. E. Turner, *"Interface Effects on Dose Distributions in Irradiated Media,"* Seventh Symposium on Microdosimetry, Oxford, UK, September 8-12, 1980.

APPENDIX A

THE OPTICAL PROPERTIES OF KAPTON: MEASUREMENT AND APPLICATIONS

THE OPTICAL PROPERTIES OF KAPTON: MEASUREMENT AND APPLICATIONS[a]

E. T. Arakawa, M. W. Williams, J. C. Ashley, and L. R. Painter[b]

Health and Safety Research Division
Oak Ridge National Laboratory
Oak Ridge, Tennessee 37830

Written for submission to: Journal of Applied Physics

ABSTRACT

The optical properties of Kapton Type H polyimide film, obtained from reflectance measurements, are presented for photon energies from 0.5 to 70 eV. Equations for the energy-loss function, with parameters fixed by the optical data, are employed to calculate mean free paths and stopping powers for low-energy electrons (100 eV to 10 keV) in Kapton. The values obtained show good agreement with those predicted by recently proposed analytical formulae for electron mean free paths and stopping powers in solid organic insulators.

PACS numbers: 78.20.Dj; 78.90.+t; 78.40.Ha

---

[a] Research sponsored jointly by the Deputy for Electronic Technology, Air Force Systems Command, under Interagency Agreement DOE No. 40-226-70 and the Office of Health and Environmental Research, U.S. Department of Energy, under contract W-7405-eng-26 with the Union Carbide Corporation.

[b] Also Department of Physics and Astronomy, University of Tennessee, Knoxville, Tennessee 37916.

INTRODUCTION

Direct measurements of the mean free paths and stopping powers of low-energy electrons in solid organic insulators, such as polystyrene and polyethylene, are difficult.[1] On the other hand, it has been known for some time that a knowledge of the optical properties of a material over an energy range that covers essentially all of the oscillator strength of the valence electrons, enables the transport properties for ionizing radiations interacting with the valence electrons to be calculated. In a recent publication[2] we used our measured values of the optical properties of polyethylene from 0.5 to 76 eV in calculations of the inelastic mean free paths and stopping powers for low-energy electrons (10 eV to 10 keV) in polyethylene. Data obtained previously on five other solid organic insulators have been utilized in the same way[3,4] and simple, analytical formulae deduced which predict mean free paths and stopping powers for electrons in solid organic insulators in the energy range from 100 eV to 10 keV. It is of great interest to check these predictions using a material for which the optical properties were not available previously over an energy range which covers essentially the whole of the oscillator strength for the valence electrons.

Kapton is a solid organic insulator with a monomeric unit of $-\!\!\left(C_{22}H_{10}N_2O_5 \right)\!\!-$. Kapton Type H polyimide film[5] is used extensively in situations demanding good electrical insulation, radiation resistance, and/or chemical resistance, particularly at high operating temperatures. At room temperature the physical properties of Kapton are similar to those of Mylar polyester film,[5] but Kapton is less affected by temperature changes and is also $\sim$50 times more resistant to radiation damage than Mylar. In fact, Kapton has been found to retain its useful properties over the wide temperature range from -269°C to +400°C. In view of its extensive use, the optical properties of Kapton, and hence a knowledge of the transport parameters for ionizing radiations in Kapton, are of particular interest. In addition, measurements of the optical properties of Kapton over an energy range which covers essentially all of the oscillator strength of the valence electrons enables a comparison to be made between the values of electron mean free paths and stopping powers obtained from the measured optical properties and those predicted from our analytical formulae. Agreement, within the limits of experimental errors, would lend some support to the claim that our analytical formulae for mean free path and stopping power apply to low-energy electrons in all solid organic insulators.

In this paper we present the optical properties of Kapton from 0.5 to 70 eV, and then use these data to calculate electron mean free paths and stopping powers in Kapton. To our knowledge the only optical data available previously, provided by the manufacturer[5] and appearing in the open literature,[6] were in the I.R. and in the vicinity of the interband absorption edge.

EXPERIMENTAL PROCEDURE

Kapton is available[5] as Type H film with nominal thicknesses from 7.6×10^{-6} m to 1.27×10^{-4} m. Such films are too thick for transmission measurements in the vacuum UV region. Furthermore, efforts to obtain Kapton films suitable for transmission measurements above the energy region of the UV absorption edge were unsuccessful. The optical properties of Kapton were thus obtained primarly from reflectance measurements, using photons ranging in energy from 0.5 eV (2500 nm) to 70 eV (17.7 nm) reflected from Kapton films stretched over a sample holder. Measurements were made with a spectrophotometer (Cary Model 14) in the 0.5 to 5.4 eV (2500 to 230 nm) range, a Seya-Namioka monochromator (McPherson Model 235) in the 2.0 to 15 eV (620 to 82.7 nm) range, and with a grazing incidence monochromator (McPherson Model 247) in the 13 to 70 eV (95.4 to 17.7 nm) range. The values obtained for the normal incidence reflectance from 0.5 to 70 eV are shown in Fig. 1.

For photon energies where the extinction coefficient, k, is essentially zero, interference patterns in the spectrum obtained by reflection were analyzed to give the refractive index, n, and the thickness of the film. Values of the normal incidence reflectance at each photon energy were calculated from n, assuming k = 0. For photon energies where k is small, but not zero, reflectance and transmittance measurements were analyzed to yield n. Transmission measurements on the thinnest Kapton films in this energy region (i.e., in the region of the ultraviolet absorption edge) were also used to obtain the values of k. Values of the normal incidence reflectance were then calculated from a knowledge of n and k. From the onset of absorption to $\sim$25 eV, the near-normal incidence reflectance was measured directly using the Seya-Namioka and grazing incidence monochromators. In the 3.0 to 5.4 eV region, structure in the normal incidence reflectance was confirmed by values obtained from reflection measurements in the Cary 14 spectrophotometer. These data were normalized at 3.0 eV. For photon energies $\gtrsim$ 25 eV, at each energy the measured reflectance as a function of the angle of incidence was least-squares fit to Fresnel's equations to yield the values of n and k. For photon energies $\lesssim$ 25 eV, this method did not yield accurate values of n and k for Kapton. In order to obtain the optical properties of Kapton over the whole energy range from 0.5 to 70 eV, the measured n and k values from 0.5 to 3.0 eV and 25 to 70 eV were combined with the values of the near-normal incidence reflectance from 0.5 to 70 eV. These data were then analyzed by a Kramers-Kronig technique which we had previously developed.[7]

The phase change on reflection, θ, is given as a function of incident photon energy, E, by

$$\theta(E) = \frac{E}{\pi} \int_0^{\infty} \frac{\ln R(E')}{(E')^2-E^2}\, dE'$$

$$= \frac{E}{\pi} \int_0^{70\,\mathrm{eV}} \frac{\ln R(E')}{(E')^2-E^2}\, dE' \qquad (1)$$

$$+ \frac{E}{\pi} \int_{70\,\mathrm{eV}}^{\infty} \frac{\ln R(E')}{(E')^2-E^2}\, dE' \quad ,$$

where $-\pi \le \theta \le 0$. The integral from 0 to 70 eV was calculated as a function of E from the near-normal incidence reflectance spectrum shown in Fig. 1. The integral from 70 eV to infinite energy is the contribution, $\Delta\theta(E)$, to the phase change on reflection due to absorption in the energy region above the limit of the experimental data. Its value at any energy E depends on the reflectance between 70 eV and infinite energy. For energies E below 70 eV, $\Delta\theta(E)$ must be a smoothly varying monotonic function of E with $d(\Delta\theta)/dE \le 0$ and $d^2(\Delta\theta)/dE^2 \le 0$. Knowing R from 0 to 70 eV, $\Delta\theta(E)$ can be calculated from Eq. 1 when n and k are known since

$$\theta(E) = \tan^{-1}[2k/(1-n^2-k^2)] \quad . \qquad (2)$$

The calculated values of $\Delta\theta$, from 0 to 3 eV and 25 to 70 eV, are shown in Fig. 2. $\Delta\theta$ was interpolated in the energy range from 3 to 25 eV by a smoothly varying function as shown in Fig. 2, and θ was then obtained by substitution back into Eq. 1. Knowledge of θ and R in the interpolated region then yielded n and k from the equations

$$n = (1-R)/(1+R-2\sqrt{R}\cos\theta)$$

and (3)

$$k = (-2\sqrt{R}\sin\theta)/(1+R-2\sqrt{R}\cos\theta) \quad .$$

This method of Kramers-Kronig analysis does not require extrapolation of the measured reflectance to higher energies. The values of n and k obtained from 3 to 25 eV are normalized to directly measured values in the adjoining energy regions, and are the same as if the Kramers-Kronig analysis had been performed by using the correct extrapolation of R to infinity. The estimated uncertainties on the values obtained for n and k are everywhere $\leq$ 6%.

DISCUSSION

Our results for Kapton are shown in Figs. 3 through 6, in the form of n and k, ε_1 and ε_2, the real and imaginary parts of the complex dielectric function $\tilde{\varepsilon}$, and the energy-loss function, $\mathrm{Im}(-1/\tilde{\varepsilon})$. As a check for consistency of these data with the results for other hydrocarbons, the sum rules for ε_2 and for $\mathrm{Im}(-1/\tilde{\varepsilon})$ are shown in Fig. 7. The effective number of electrons, n_{eff}, per monomeric unit of Kapton has been calculated as a function of incident photon energy from the well-known sum rules,[8]

$$\int_0^E E'\varepsilon_2(E')dE' = \frac{2\hbar^2\pi^2 N_o e^2}{m} \; n_{eff}$$

and

$$\int_0^E E'\mathrm{Im}\left(\frac{-1}{\tilde{\varepsilon}(E')}\right)dE' = \frac{2\hbar^2\pi^2 N_o e^2}{m} \; n_{eff} \quad ,$$

where N_o is the number of monomeric units $\leftarrow C_{22}H_{10}N_2O_5 \rightarrow$ per unit volume and e and m are the charge and mass, respectively, of an electron. By comparison with other hydrocarbons,[2,9] the effective number of electrons participating up to 70 eV should be ∿ 93% of the number of valence electrons in the monomeric unit. For Kapton the number of valence electrons is 138 and hence we anticipate an n_{eff} of 128 at 70 eV. It is seen that $n_{eff} \simeq 129$ in Fig. 7 -- well within the experimental uncertainty.

APPLICATIONS

A. Electron Inelastic Mean Free Paths

Values of inelastic mean free paths for electrons with energies from 100 eV to 10 keV in Kapton were calculated from the optical data as described previously.[3,10] Briefly, a model for the energy-loss function was employed which requires optical data to fix certain adjustable parameters. The values obtained from the optical data are shown in Fig. 8.

We have predicted[3,4,10] that the mean free path, Λ, for solid organic insulators is given by

$$1/\Lambda = (\rho N/M\mathcal{E})\cdot(13.6\,ln\,\mathcal{E}-17.6-1400/\mathcal{E}) \quad , \qquad (4)$$

where Λ is given in Å when the density ρ is in g/cm^3, the molecular weight M is in g/mol, the electron energy $\mathcal{E}$ is in eV, and N is the number of valence electrons per molecule or monomeric unit. This formula was obtained by calculating Λ from the existing optical data for six solid organic insulators for which the optical data covered essentially the whole of the oscillator strength of the valence electrons. Equation 4 was then the best fit to the Λ values for the six materials. This has been termed a "universal" curve for Λ for solid organic insulators. The availability of the optical data for Kapton over a large fraction of the oscillator strength of the valence electrons gives us an opportunity to test the "universal" curve for Λ. Figure 8 shows the values of Λ from 100 eV to 10 keV predicted for Kapton from Eq. 4. It is seen that there is excellent agreement between the two curves for Λ. The difference ranges from 5% at 100 eV to $< 3\%$ at 10 keV. This is well within the accuracy claimed for the predictions of Eq. 4.

It is anticipated that Eq. 4 should also predict the mean free paths of electrons in liquid organic insulators and in water. Confirmation must await the availability of optical data to higher energies.

B. Stopping Powers

In a similar manner the stopping power for low-energy electrons due to interactions with the valence electrons in Kapton can be calculated from the measured optical properties.[2,4]

It has been predicted[4] that the contribution of the valence electrons, S_v, to the stopping power of a solid organic insulator is given by

$$S_v[\mathrm{eV}/\mathring{\mathrm{A}}] = (\rho N/M\mathcal{E})\cdot(8.26\times10^{2}\,\ln\mathcal{E} - 2.61\times10^{3} - 3.03\times10^{4}/\mathcal{E}) \quad , \qquad (5)$$

for $100\ \mathrm{eV} \leq \mathcal{E} \leq 10\ \mathrm{keV}$, in terms of the same material parameters employed in Eq. (4).

The values calculated for S_v, both from the optical data for Kapton and from Eq. (5) are shown in Fig. 9. It is seen that there is satisfactory agreement, with 9% difference at 100 eV, 3% at 300 eV and less than 1% at 10 keV.

REFERENCES

1. M. P. Seah and W. A. Dench, Surf. Interface Anal. 1, 2-11 (1979).
2. L. R. Painter, E. T. Arakawa, M. W. Williams, and J. C. Ashley, Radiat. Res. 83, 1-8 (1980).
3. J. C. Ashley and M. W. Williams, Radiat. Res. 81, 364-373 (1980).
4. J. C. Ashley, IEEE Trans. Nucl. Sci. To be published.
5. Manufactured by E. I. du Pont de Nemours and Company.
6. W. J. Wrasidlo, J. Polym. Sci.: Polym. Phys. Ed. 11, 2143-2152 (1973);
7. E. T. Arakawa and M. W. Williams, J. Phys. Chem. Solids 29, 735-744 (1968).
8. See for example H. Ehrenreich, H. R. Philipp, and B. Segall, Phys. Rev. 132, 1918-1928 (1963); P. Nozières and D. Pines, Phys. Rev. 113, 1254-1267 (1959).
9. T. Inagaki, E. T. Arakawa, R. N. Hamm, and M. W. Williams, Phys. Rev. B 15, 3243-3253 (1977).
10. M. W. Williams and J. C. Ashley, Proc. VI Int. Conf. Vac. UV Rad. Phys., Univ. Virginia, Charlottesville, Va., 2-6 June 1980, Vol I-67 pp. 1-3.

FIGURE CAPTIONS

Fig. 1 Normal incidence reflectance of Kapton as a function of incident photon energy.

Fig. 2 Contribution to the phase angle due to absorption above 70 eV as a function of incident photon energy for Kapton film.

Fig. 3 The optical constants n and k of Kapton as a function of incident photon energy.

Fig. 4 The extinction coefficient, k, of Kapton as a function of incident photon energy.

Fig. 5 The dielectric functions, ε_1 and ε_2, of Kapton as a function of incident photon energy.

Fig. 6 The energy loss function $\mathrm{Im}(-1/\tilde{\varepsilon})$ of Kapton as a function of incident photon energy.

Fig. 7 The effective number of electrons per monomeric unit of Kapton $-\!\!(\ C_{22}H_{10}N_2O_5\ )\!\!-$ as a function of incident photon energy.

Fig. 8 Comparison of the mean free path of Kapton calculated as a function of electron energy from the optical data and from the universal relation given by Eq. 4.

Fig. 9 Comparison of the valence electron contribution to the stopping power of Kapton calculated as a function of electron energy from the optical data and from the universal relation given by Eq. 5.

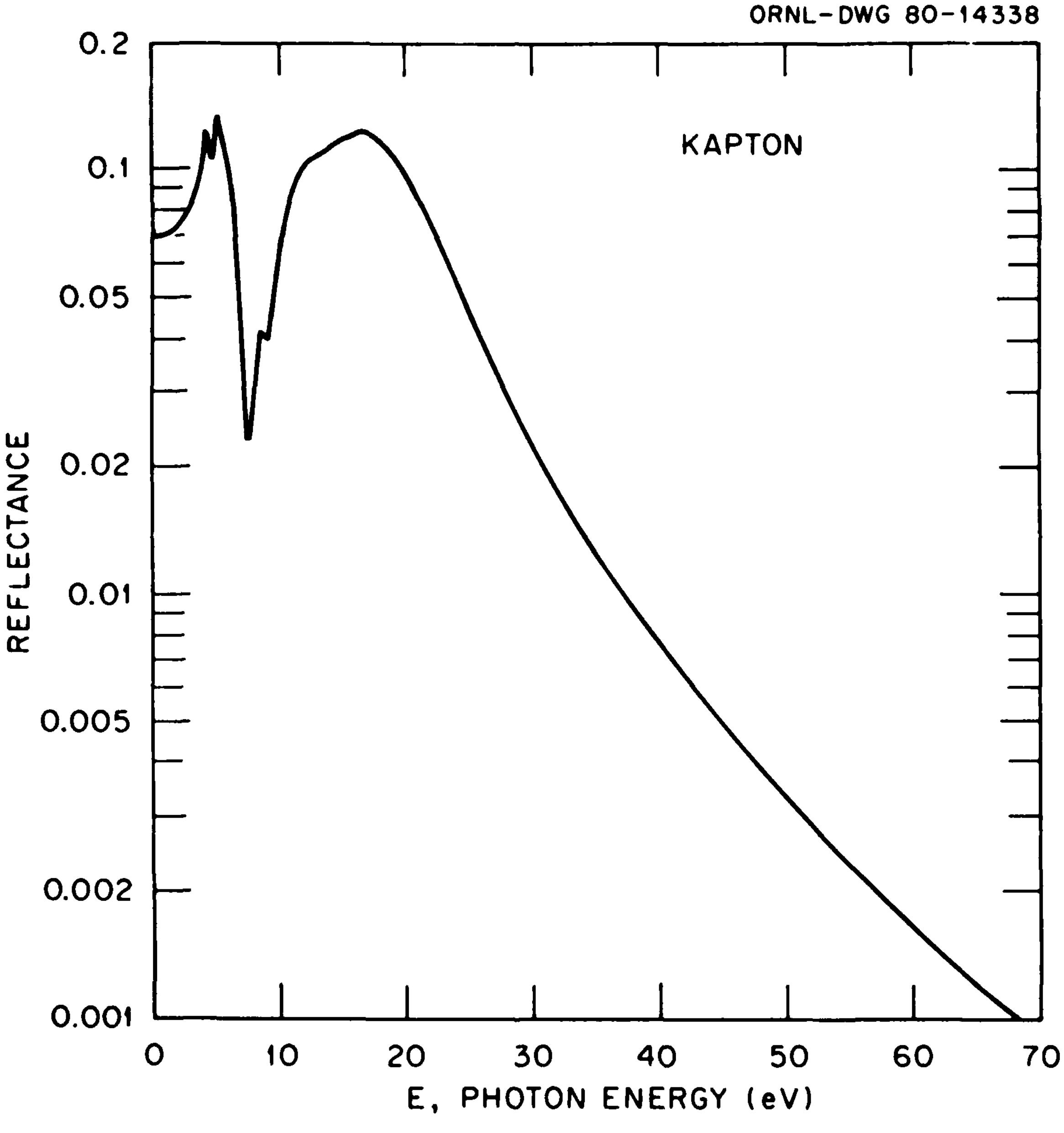
ORNL-DWG 80-14338
KAPTON
REFLECTANCE
0.2
0.1
0.05
0.02
0.01
0.005
0.002
0.001
0
10
20
30
40
50
60
70
E, PHOTON ENERGY (eV)

FIGURE 1

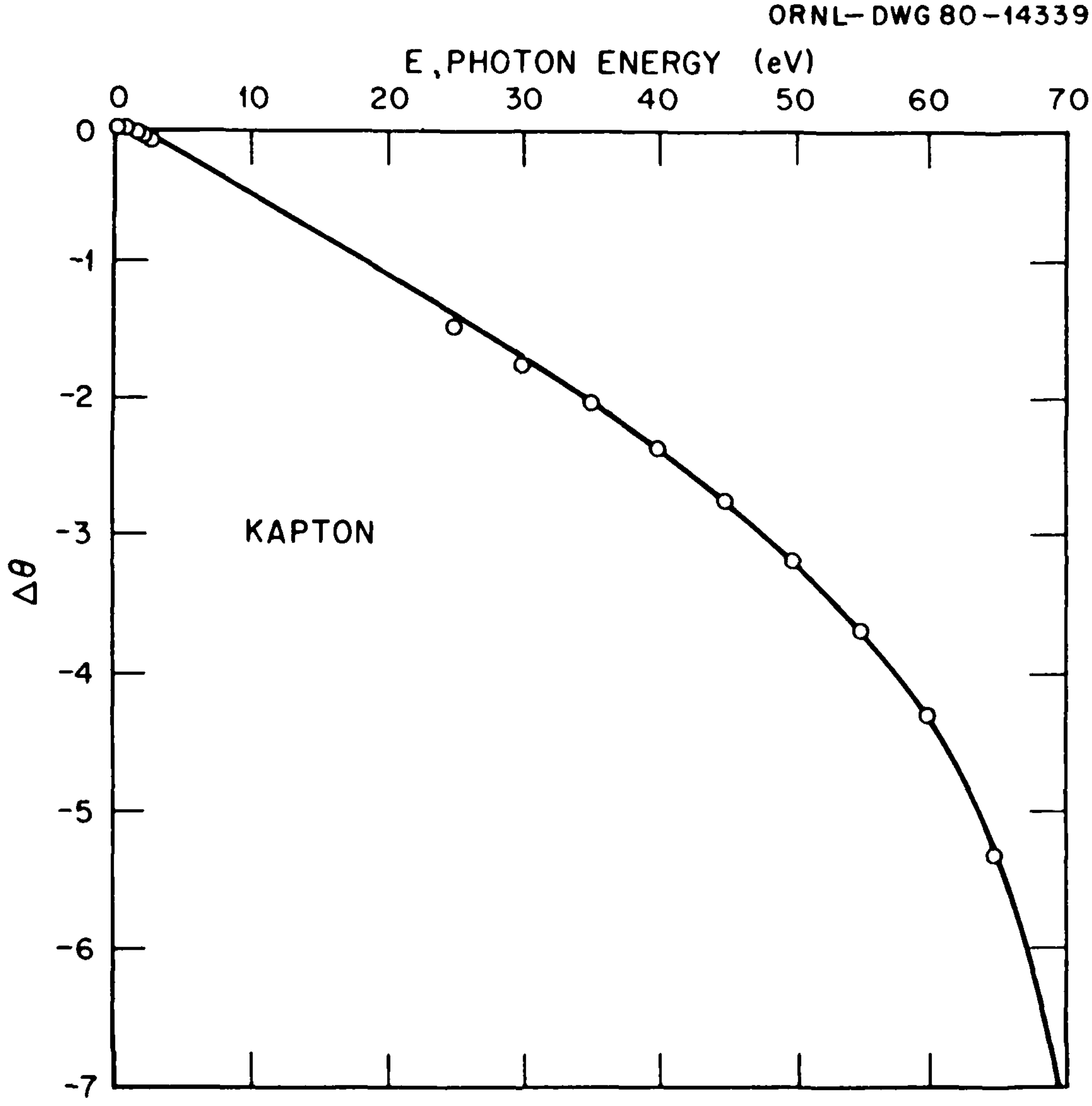
ORNL-DWG 80-14339
E, PHOTON ENERGY (eV)
0
10
20
30
40
50
60
70
0
-1
-2
-3
-4
-5
-6
-7
Δθ
KAPTON

FIGURE 2

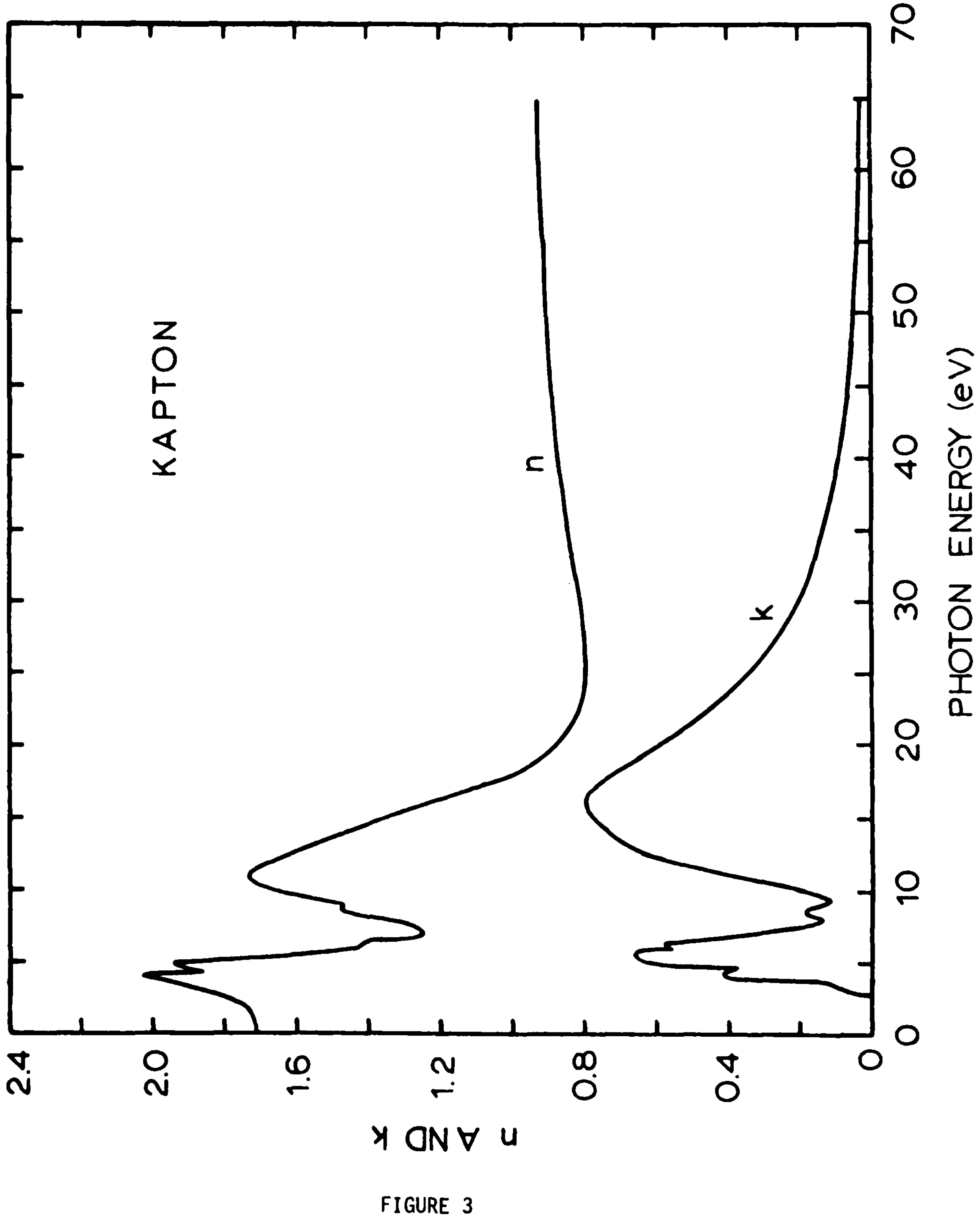
KAPTON
n
k
n AND k
2.4
2.0
1.6
1.2
0.8
0.4
0
0
10
20
30
40
50
60
70
PHOTON ENERGY (eV)

FIGURE 3

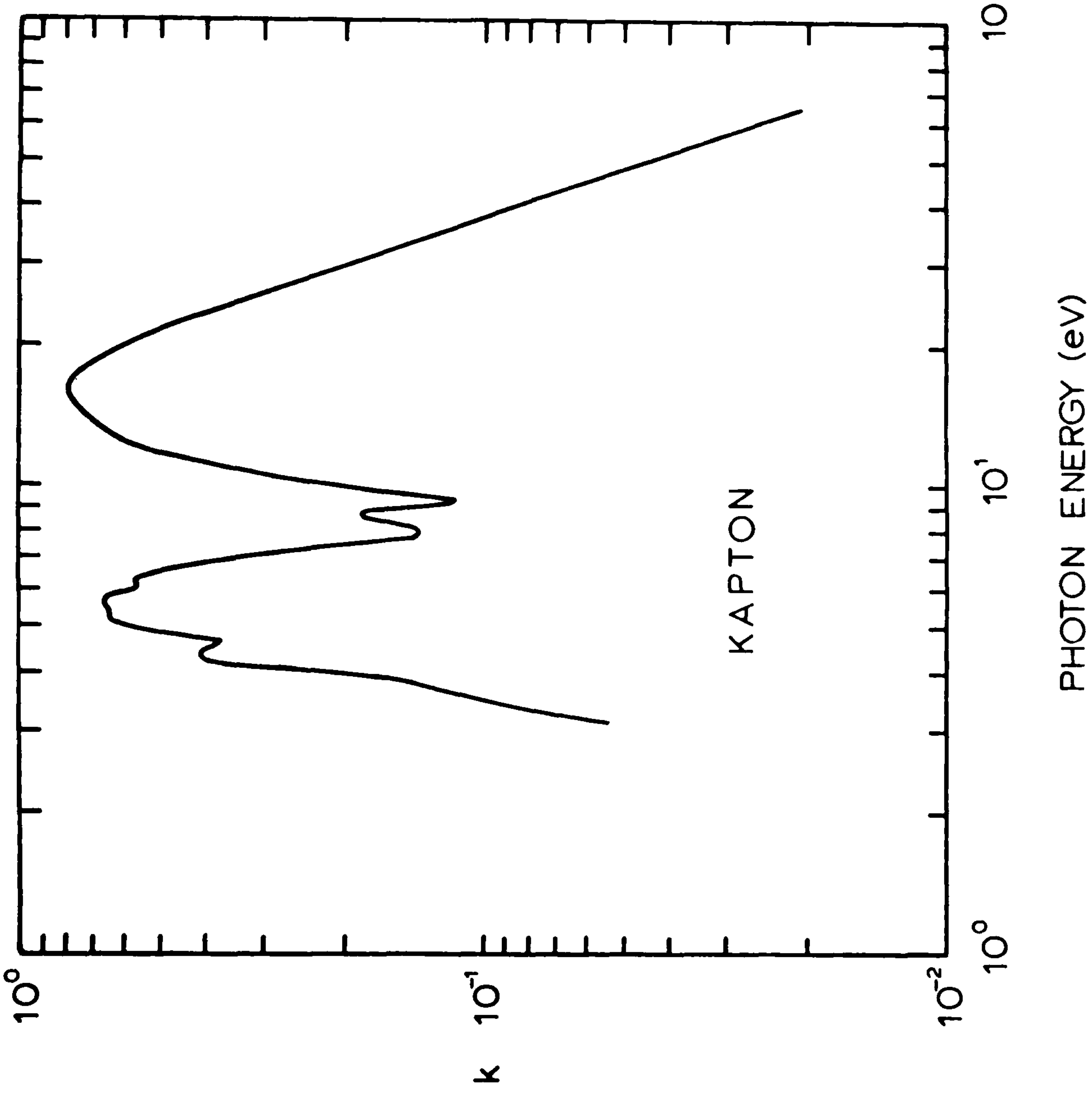

FIGURE 4

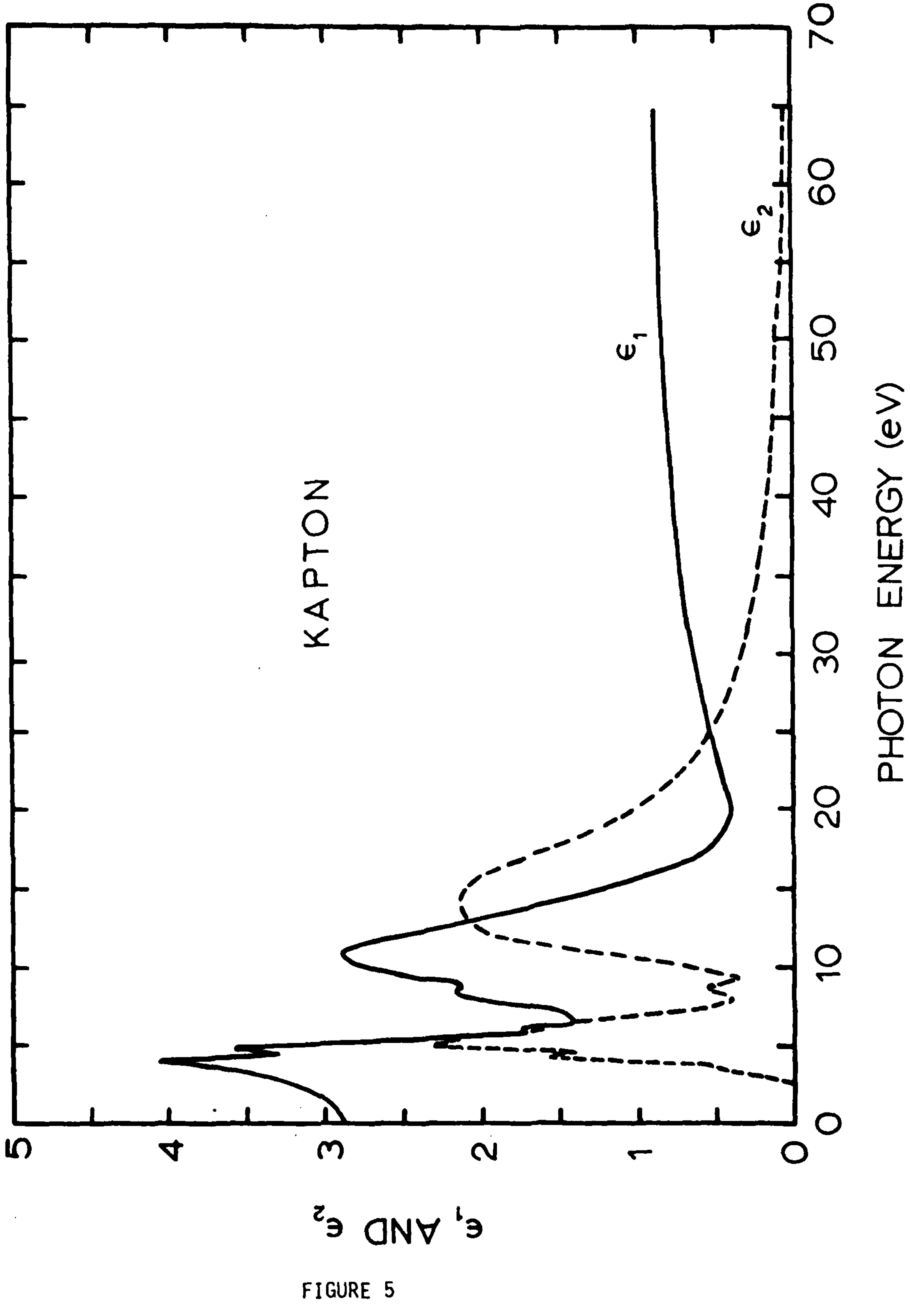
KAPTON
ϵ_1
ϵ_2
PHOTON ENERGY (eV)
0
10
20
30
40
50
60
70
ϵ_1 AND ϵ_2
0
1
2
3
4
5

FIGURE 5

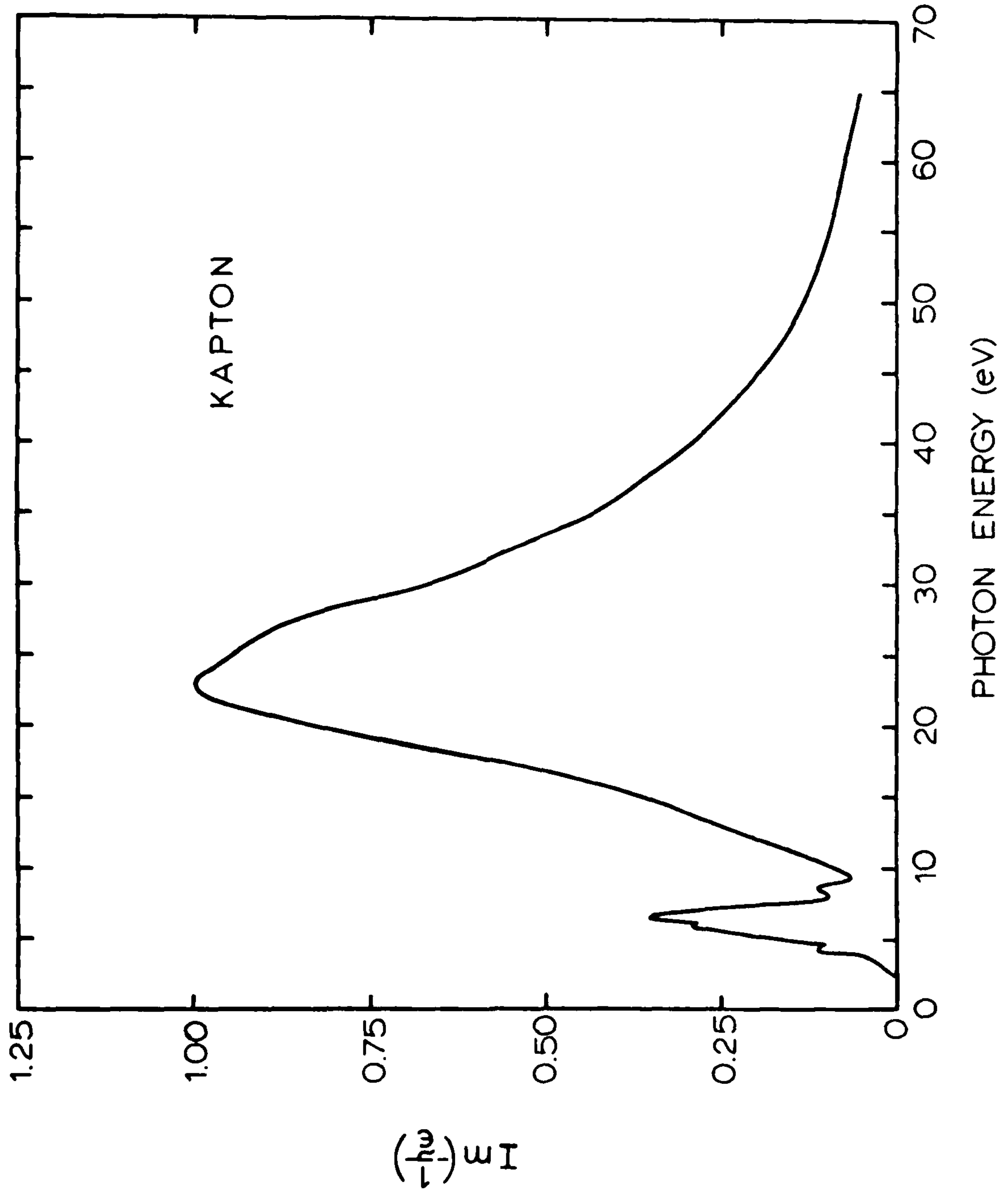
KAPTON
PHOTON ENERGY (eV)
0
10
20
30
40
50
60
70
Im(-1/ε)
0
0.25
0.50
0.75
1.00
1.25

FIGURE 6

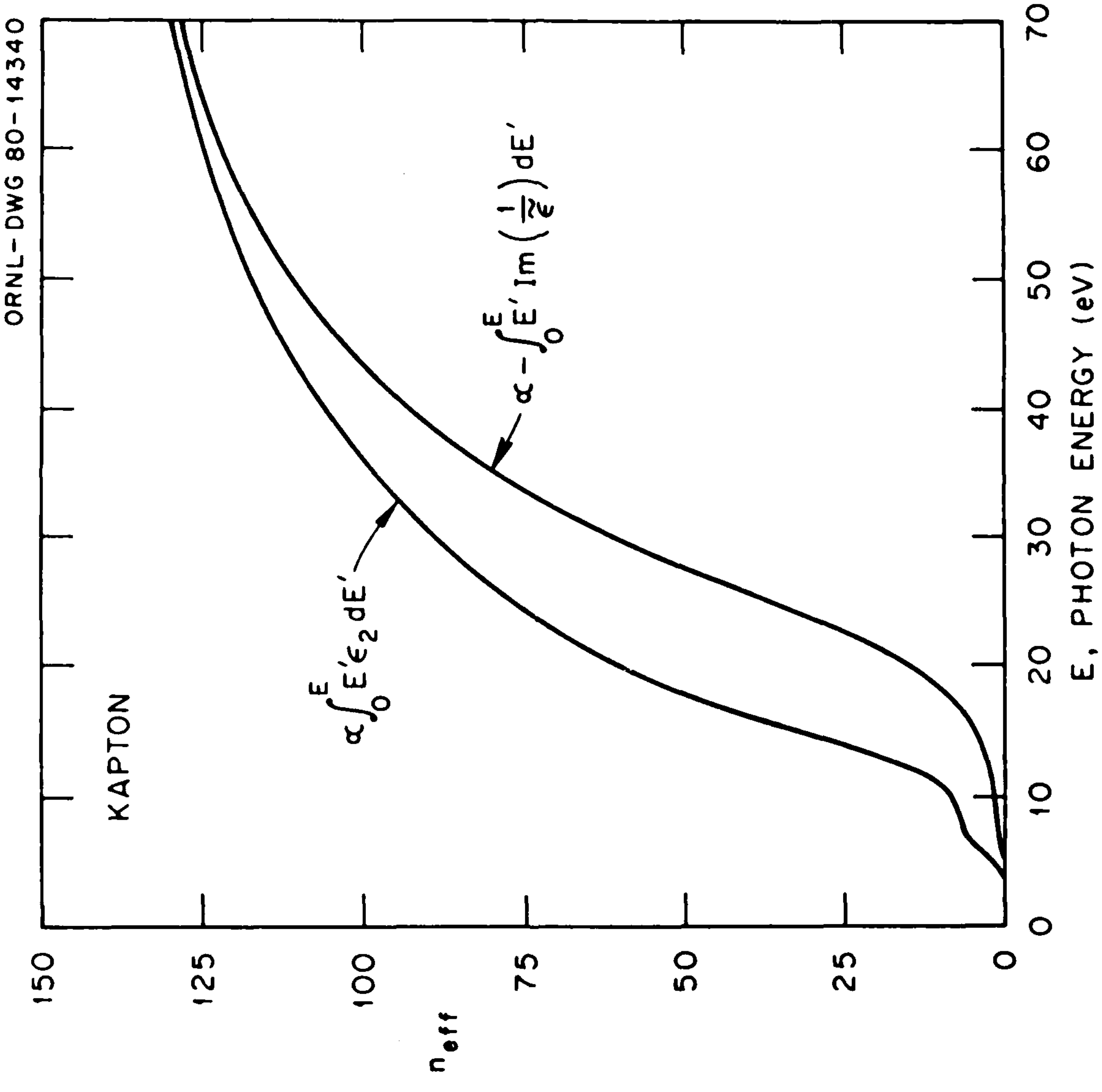
ORNL-DWG 80-14340
KAPTON
$\propto \int_0^E E'\epsilon_2\,dE'$
$\propto -\int_0^E E'\,\mathrm{Im}\left(\frac{1}{\tilde{\epsilon}}\right)dE'$
n_{eff}
150
125
100
75
50
25
0
0
10
20
30
40
50
60
70
E, PHOTON ENERGY (eV)

FIGURE 7

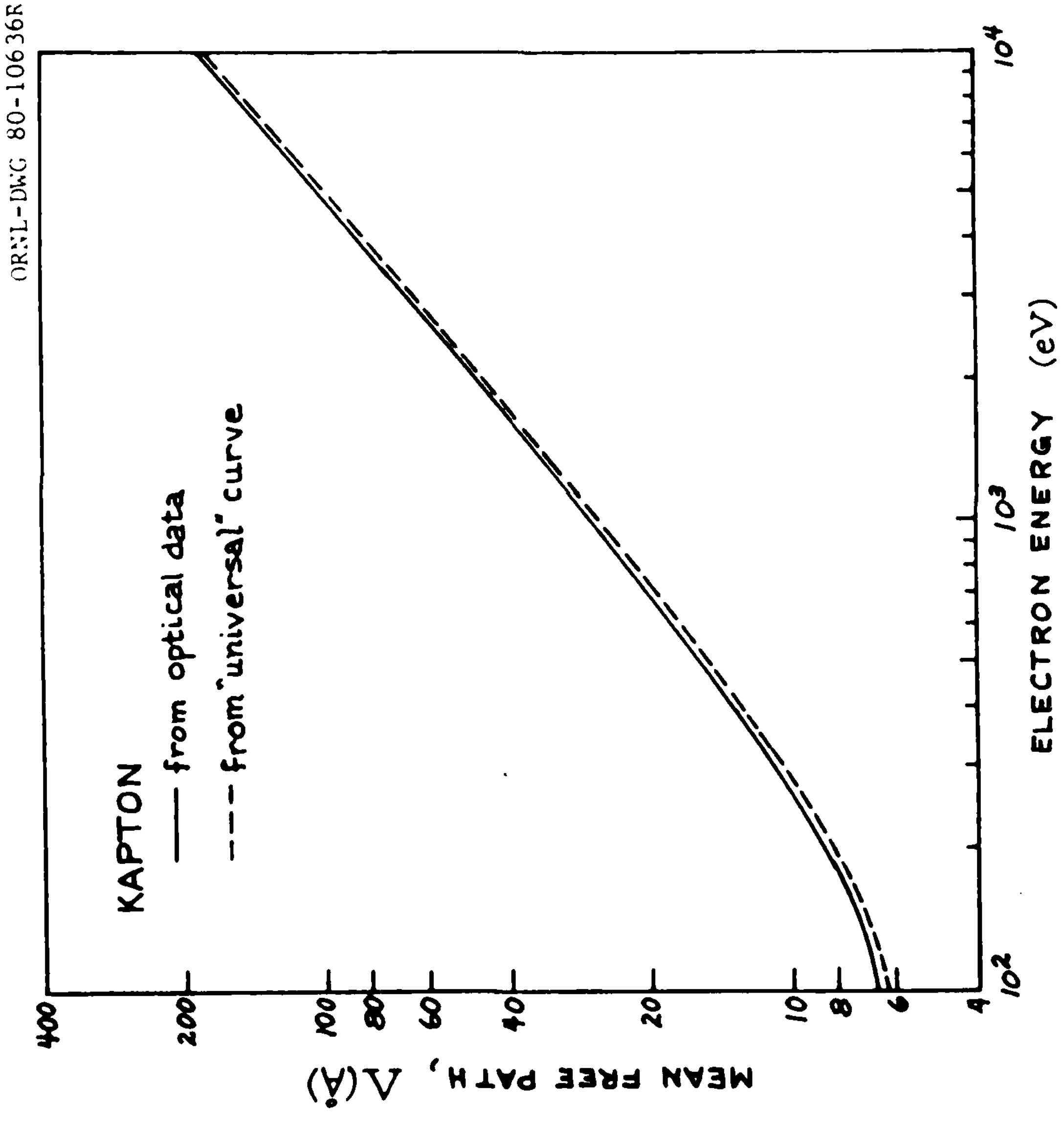
ORNL-DWG 80-10636R
KAPTON
—— from optical data
- - - from 'universal' curve
ELECTRON ENERGY (eV)
10^2
10^3
10^4
MEAN FREE PATH, Λ(Å)
4
6
8
10
20
40
60
80
100
200
400

FIGURE 8

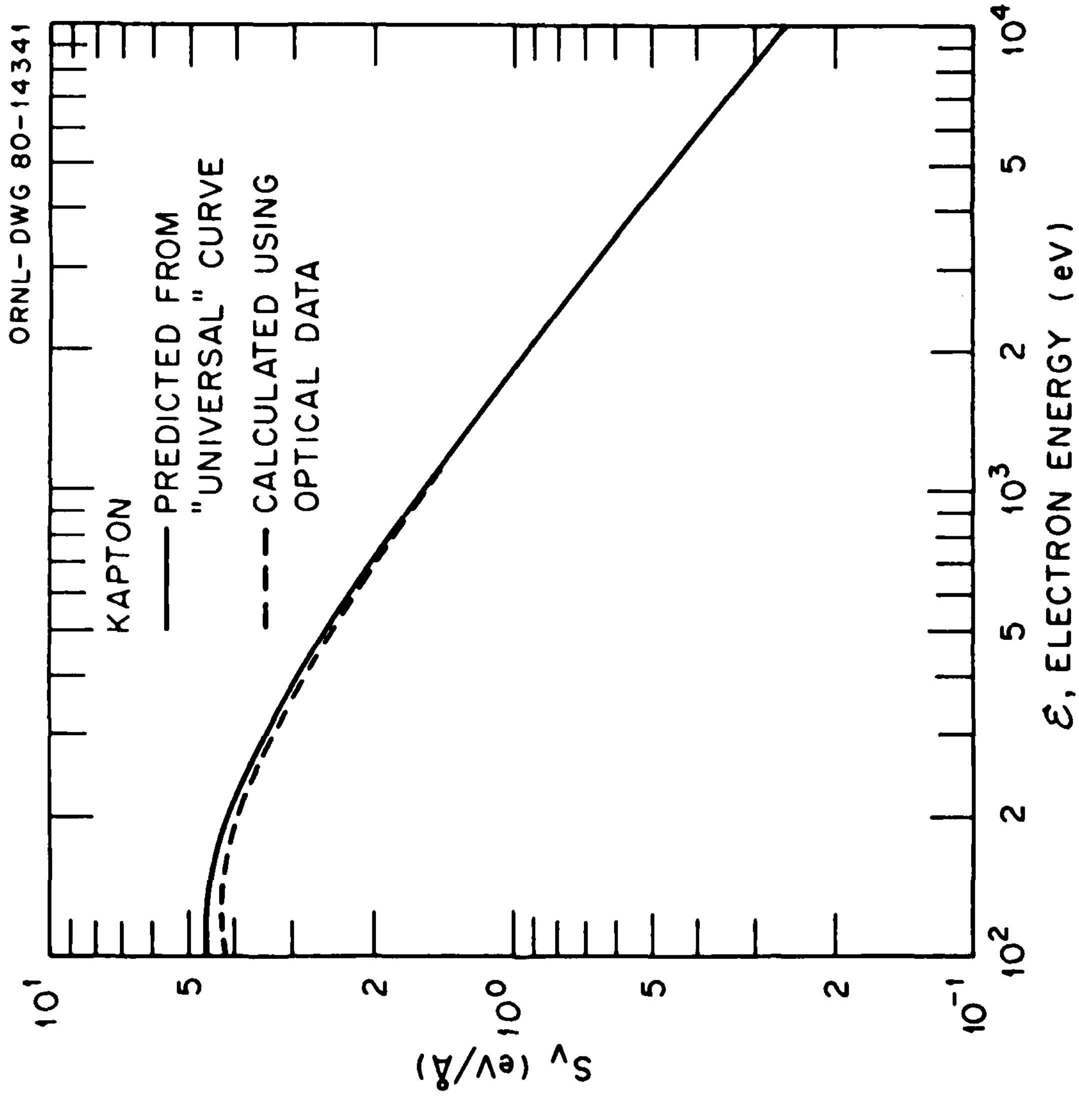
ORNL-DWG 80-14341
KAPTON
PREDICTED FROM "UNIVERSAL" CURVE
CALCULATED USING OPTICAL DATA
10^1
5
2
10^0
5
2
10^{-1}
S_V (eV/Å)
10^2
2
5
10^3
2
5
10^4
ℰ, ELECTRON ENERGY (eV)

FIGURE 9

APPENDIX B

INELASTIC INTERACTIONS OF LOW-ENERGY ELECTRONS WITH ORGANIC SOLIDS: SIMPLE FORMULAE FOR MEAN FREE PATHS AND STOPPING POWERS

INELASTIC INTERACTIONS OF LOW-ENERGY ELECTRONS WITH ORGANIC SOLIDS: SIMPLE FORMULAE FOR MEAN FREE PATHS AND STOPPING POWERS[1]

J. C. Ashley

Health and Safety Research Division
Oak Ridge National Laboratory
Oak Ridge, Tennessee 37830

ABSTRACT

A theoretical description of the inelastic interactions of low-energy electrons ($E \leq 10$ keV) with solid organic insulators is presented. The response of the valence electrons to energy and momentum transfers is inferred from a model for the energy-loss function with parameters fixed by optical data. With this model energy-loss function, inverse mean free path and stopping power due to interactions with the valence electrons are calculated for several organic solids. Contributions to the inverse mean free path and stopping power due to K-shell ionization in carbon, nitrogen, and oxygen are obtained from theoretical atomic generalized oscillator strengths. Simple, analytical formulae are deduced which allow predictions of mean free paths and stopping powers for electrons in the energy range $100\ \text{eV} \leq E \leq 10$ keV to be made for a large group of organic solids.

I. INTRODUCTION

Knowledge of the inelastic interactions of electrons with solids is important in a wide variety of applications which involve energy deposition in matter. Information generated by our group[2] on electron mean free paths and stopping powers is available for electron energies ≤ 10 keV for several metals and semiconductors important in electronics applications. Theoretical calculations of these transport parameters were recently presented for the organic insulators polystyrene[3] and polyethylene.[4] Such material by material studies are, however, rather time consuming. It would be useful to be able to generalize these results to apply, if only approximately, to a broad group of materials. The purpose of this paper is to describe simple analytical formulae for mean free paths and stopping powers for electrons of energies from 100 eV to 10 keV in solid organic insulators.

II. THEORETICAL MODEL

The basic equation required for mean free path or stopping power calculations is that for the differential inverse mean free path (DIMFP),[5]

$$\frac{d\mu}{d(\hbar\omega)} = \frac{1}{\pi a_0 E} \int_{q-}^{q+} \frac{dq}{q} \, \mathrm{Im}[-1/\varepsilon(q,\omega)] \ , \qquad (1)$$

which gives the probability per unit distance per unit energy for an electron of energy E to suffer an energy loss in the interval from $\hbar\omega$ to $\hbar\omega + d(\hbar\omega)$. The DIMFP is given by an integral over possible momentum transfers, $\hbar q$, to a medium described by the dielectric response function $\varepsilon(q,\omega)$. The medium is assumed to be homogeneous and isotropic, the integration limits are given by $\hbar q_{\pm} = \sqrt{2m}\left[\sqrt{E} \pm \sqrt{E-\hbar\omega}\right]$, and $a_0 \equiv \hbar^2/me^2$ is the Bohr radius. The inverse mean free path μ and stopping power S are given by

$$\mu(E) = \int_0^{0.583E} d(\hbar\omega)\; d\mu/d(\hbar\omega) \;, \tag{2}$$

and

$$S(E) = \int_0^{0.583E} d(\hbar\omega)\; \hbar\omega\; d\mu/d(\hbar\omega) \;, \tag{3}$$

where the factor 0.583 in the upper limit of these integrals accounts, in an approximate fashion, for the influence of exchange between the incident electron and electrons in the medium.[6]

Since the dielectric response function is usually not known in detail for a given material, model calculations must be employed to *determine* $\epsilon(q,\omega)$ *or, as required in Eq. (1),* the energy-loss function $\mathrm{Im}[-1/\epsilon(q,\omega)]$. The model used here involves representing $\mathrm{Im}[-1/\epsilon(q,\omega)]$ by a sum of Drude-type functions with each term in the sum involving three adjustable parameters.[7,8] The parameters are determined for a specific material by fitting the model energy-loss function for $q=0$ to the optical energy loss function $\mathrm{Im}[-1/\epsilon(0,\omega)]$ as determined by optical data for that material. Optical data for photon energies up to ∿80 eV for polyethylene, polystyrene, DNA (deoxyribonucleic acid), BPA (bovine plasma albumin), adenine, and guanine were used to specify the model energy-loss function for these six solid organic insulators. Complete references to the optical data are given in Ref. 8. The energy-loss function determined in this manner describes only the response of the valence electrons; the contributions to μ and S from ionization of inner shells is treated separately and will be discussed below.

III. MEAN FREE PATHS

For the six organic insulators for which sufficient optical data were available, inverse mean free paths were calculated from Eqs. (1) and (2). We found[8] that the contribution to the inverse mean free path due to interactions with the valence electrons $\mu_v(E)$, divided by the valence electron density n_v, for all six materials could be represented to better than ±10% by a single function of energy for $100\ \text{eV} \leq E \leq 10\ \text{keV}$. The calculations described in Ref. 8 were repeated with electron exchange included as discussed below Eq. (3). In addition, an increase in the effective number of valence electrons by a factor of ~ 1.05 due to oscillator strength coupling between core and valence electrons, as noted earlier in polystyrene[9] and polyethylene,[4] has been incorporated in the expressions for both μ_v and S_v. With these changes, I find

$$\mu_v[\mathring{A}^{-1}]/n_v[\mathrm{au}] = (152\ln E - 198 - 1.57\times10^4/E)/E \equiv f_v(E) , \qquad (4)$$

where μ_v is in units of reciprocal Angstroms, E is in electron volts, and n_v is in atomic units. For simplicity, the factor 1.05, discussed above has been included in the numerical coefficients in Eq. (4). The use of this factor results in a slight overestimate of μ_v and S_v. This point is discussed further in Section V.

Values of n_v for a selection of organics which contain only nitrogen and oxygen in addition to carbon and hydrogen are given in Table I along with relevant physical properties and conversion factors.

Contributions to the total inverse mean free path due to ionization of K shells in carbon, nitrogen, and oxygen have been calculated from theoretical atomic generalized oscillator strengths (GOS's). The results for carbon and oxygen were used earlier in tables of electron mean free paths in polystyrene[3] and silicon dioxide.[10] The values for nitrogen were derived from McGuire's GOS values.[11] The ionization cross sections per K shell σ_K, in atomic units, are listed in Table II as functions of incident electron energy. The total inverse mean free path is given as a function of electron energy by the sum of the valence electron contribution, Eq. (4), and K-shell ionization contribution as

$$\mu[\text{Å}^{-1}] = n_v[\text{au}]f_v(E) + 1.89\sum_i \sigma_{K,i}[\text{au}]n_{K,i}[\text{au}] \;, \tag{5}$$

where the sum is over atomic K shells for carbon, nitrogen, and oxygen and $n_{K,i}$ is the number of K shells per unit volume (from Table I). For each material in Table I the contribution to μ from K-shell ionization is $\leq 1\%$. Thus electron mean free paths in these solids, $\Lambda \equiv 1/\mu$, are determined mainly by interactions with the valence electrons, Eq. (4), and the inner-shell contributions may be omitted. If the valence electron density is expressed in terms of the density ρ in g/cm^3, the number of valence electrons per molecule or monomeric unit N, and the molecular weight M in g/mol, the inverse mean free path from Eq. (4) may be written

$$1/\Lambda[\text{Å}] = (\rho N/ME)\cdot(13.6\,\ell n E - 17.6 - 1400/E) \;, \tag{6}$$

where E is in electron volts. This equation is expected to predict values of electron mean free paths for $100\text{ eV} \leq E \leq 10\text{ keV}$ to within ±10% for organic insulators. Mean free paths calculated from Eq. (6) for $E \gtrsim 200$ eV are $\lesssim 3\%$ larger than those predicted earlier for electrons in polystyrene,[3] and $\lesssim 6\%$ larger for polyethylene,[4] based on a more complicated model for the energy-loss function. Comparison of our earlier theoretical result with the meager experimental data on organics is given in Ref. 8.

Mean free paths calculated from Eq. (6) are <5% smaller than those predicted by Eq. (9) of Ref. 8 for E $\gtrsim$200 eV.

IV. STOPPING POWERS

The model described above to determine the energy-loss function has been used to calculate the contribution of valence electrons to the mean energy loss per unit path length for electrons or the stopping power of the solid for electrons. I find that contributions to the stopping powers, S_v, as determined by calculations for polystyrene, polyethylene, guanine, and adenine, can be summarized by the simple result

$$S_v[\mathrm{eV}/\mathring{A}] = (\rho N/ME)\cdot(8.26\times10^2 \ln E - 2.61\times10^3 - 3.03\times10^4/E) \ , \tag{7}$$

for 100 eV$\leq$E$\leq$10 keV, in terms of the same material parameters employed in Eq. (6). S_v from Eq. (7) may slightly overestimate the valence electron contribution to stopping power. This is discussed in Section V.

Ionization of inner shells of the atoms in a medium can make significant contributions to the stopping power for electron energies less than 10 keV. If we restrict our attention to organics containing only carbon, nitrogen, oxygen, and hydrogen, a group which includes many of the important materials used in electronics applications, we need to consider only K-shell ionization. The contributions to the stopping power due to K-shell ionization by electrons have been calculated from GOS values as described previously.[3] Values of s_K, the stopping power per K shell per unit volume, shown in Table II, were extracted from Ref. 3 for carbon and from Ref. 10 for oxygen. The values of s_K for nitrogen were derived from McGuire's GOS tables.[11]

Given the expression for S_v, Eq. (7), and $s_{K,i}$, where the subscript i may represent carbon, nitrogen, or oxygen, the total stopping power is given by

$$S[\mathrm{eV/\mathring{A}}] = S_v[\mathrm{eV/\mathring{A}}] + 51.4 \sum_i n_{K,i}[\mathrm{au}] s_{K,i}[\mathrm{au}] \;, \tag{8}$$

where n_K, the number of K shells per unit volume, may be obtained from Table I. The numerical factor in front of the summation sign converts the sum, expressed in atomic units, to units of eV/Å. Stopping powers calculated from Eq. (8) are <5% smaller than the earlier results for polystyrene[3] for $E \geq 300$ eV and ∿15% smaller at $E = 100$ eV. For polyethylene[4] Eq. (8) predicts values ∿3% smaller at $E = 10$ keV, increasing to ∿20% smaller at 100 eV, than our previous tabulated values. The differences in the polyethylene values are due, in part, to neglect of exchange in our earlier tabulation.[4] For polyethylene and polystyrene, Eq. (8) predicts stopping powers which agree within 2% at $E = 10$ keV with existing tabulations[12,13] for $E \geq 10$ keV.

Equation (8) has been used to predict stopping powers for anthracene, Bakelite, Makrolon, Plexiglas (same chemical composition as Lucite, Perspex, PMMA resist), Mylar, cellophane, and two types of nylon. In all cases the stopping powers at 10 keV agree with tabulated values[12,13] to within 2%. Stopping powers for Kapton have also been predicted, but no tabulated values are available for comparison. The K-shell contributions to the stopping powers for these materials accounted for ≤10-15% of the total stopping power for $E \leq 10$ keV. The stopping powers of some of these materials are displayed in Table III. It is interesting that Kapton, Mylar, and Bakelite, which are quite different in chemical composition, are predicted to have almost identical stopping powers for the densities shown in Table I. Note also that S, Eq. (8), is linear in ρ and thus scales easily for the same material at a different density.

In Fig. 1 we show $S' \equiv S/\rho$ times electron energy as a function of electron energy for Nylon 6,6, Mylar, and Plexiglas. The solid curves are the predictions of this study; the dashed curves are from Brandt's tabulation.[14] Brandt's results agree quite well with other tabulations[12,13] for $E \geq 10$ keV and fall $\sim$5-15% below my predictions at E = 256 eV.

For some purposes it may be useful to have a simple analytical expression for s_K rather than the tabular values given in Table II. If E_K is the binding energy of the K-shell electrons, then I define U_K by $U_K \equiv E/E_K$. The values for s_K[au] in Table II were fit by an expression of the form

$$s_K[\mathrm{au}]E_K[\mathrm{au}] = \frac{\ln U_K}{U_K^p}\,(a - b/U_K + c/U_K^2)\ . \qquad (9)$$

The values determined for a, b, c, and p and the K-shell binding energies are given in Table IV. As shown in Table IV, Eq. (9) reproduces the values of s_K from Table II to better than 4% for $U_K \geq 1.5$. Since the total inner-shell contribution to the stopping power is $\lesssim$10-15% for the materials under discussion here, the use of Eq. (9) rather than s_K from Table II changes the total stopping power by <1%. For $U_K < 1.5$, near threshold, larger deviations from the values in Table II are predicted by Eq. (9). However, the values of s_K are so small in this region that even a factor of two or three difference produces a negligable effect on the total stopping power.

It is known that cross sections for K-shell ionization by electrons satisfy simple scaling laws[14] (i.e., $\sigma_K E_K^2$ should be a universal function of U_K). Theory indicates that a similar scaling law should hold for s_K and that $s_K E_K$ should be a function only of U_K for all atoms. With the values of s_K for the three elements from Table II and the functional form given by Eq. (9), I find that

$$s_K[\mathrm{au}]E_K[\mathrm{au}] = \frac{\ln U_K}{U_K}\,(9.91 - 13.0/U_K + 3.13/U_K^2)\ , \qquad (10)$$

will reproduce the Table II values of s_K for carbon, nitrogen, and oxygen to within 7% for $U_K \geq 2.5$, within 20% for $1.2 \leq U_K < 2.5$, and within a factor of ~2 for $U_K < 1.2$. The discussion following Eq. (9) is also appropriate here; the use of Eq. (10) instead of the values from Table II should lead to differences of ≲1% in the total stopping power.

V. CONCLUSIONS

I have presented simple analytical expressions for predicting mean free paths and stopping powers for electrons in organic insulators which should be useful in studies of energy deposition in some insulating materials used in electronics applications. The result for the stopping power may not be restricted to insulators since the presence of a band gap is de-emphasized by the term $\hbar\omega$ in the integral for S [see Eq. (3)]. In addition, all the formulae may apply to organic liquids as well as solids.

A further comment is nescessary about the factor 1.05 included in Eqs. (4) and (7). In the optical limit, q=0, the total oscillator strength for K-shell ionization corresponds to less than two electrons per K shell

(1.72 for C, 1.66 for N and O). The valence electron density was increased by a factor η so that the energy-loss sum rule, $\int_0^\infty d\omega\ \omega\ \mathrm{Im}[-1/\varepsilon(q,\omega)] = 2\pi^2 n$, yields the correct total electron density n. For q=0, $\eta \gtrsim 1.05$ for the materials in Table I. If η were independent of q, then μ_v and S_v would be increased by that same factor. In fact, η decreases to a value close to one for large q so a different correction is required in the energy-loss function at each value of q. The results for μ_v and S_v would then be multiplied by an energy-dependent, effective value of $\eta = \eta_{eff}(E) \lesssim 1.05$. Thus the stopping powers and inverse mean free paths given in this paper may be overestimated by a few percent, with larger overestimates occuring at the higher energies. This point and a more detailed discussion of stopping power calculations for organic insulators and the extension of this work to organic materials other than solid organic insulators will be presented elsewhere.[16]

REFERENCES

[1] Research sponsored jointly by the Deputy for Electronic Technology, Air Force Systems Command, under Interagency Agreement DOE No. 40-266-70 and the Office of Health and Environmental Research, U.S. Department of Energy, under contract W-7405-eng-26 with the Union Carbide Corporation.

[2] J. C. Ashley, C. J. Tung, R. H. Ritchie, and V. E. Anderson, *IEEE Trans. Nucl. Sci.* NS-23, 1833-1837 (1976), and references contained therein.

[3] J. C. Ashley, C. J. Tung, and R. H. Ritchie, *IEEE Trans. Nucl. Sci.* NS-25, 1566-1570 (1978); J. C. Ashley, C. J. Tung, R. H. Ritchie, and V. E. Anderson, "Inverse Mean Free Path, Stopping Power, CSDA Range, and Straggling in Polystyrene for Electrons of Energy $\leq$ 10 keV," Air Force Report RADC-TR-78-32 (February 1978).

[4] L. R. Painter, E. T. Arakawa, M. W. Williams, and J. C. Ashley, *Radiation Research* (to be published).

[5] J. Lindhard, *K. Dan. Vidensk. Selsk. Mat.-Fys. Medd.* 28, No. 8, 1-57 (1954); R. H. Ritchie, *Phys. Rev.* 114, 644-654 (1959).

[6] R. H. Ritchie (private communication).

[7] J. C. Ashley, J. J. Cowan, R. H. Ritchie, V. E. Anderson, and J. Hoelzl, *Thin Solid Films* 60, 361-370 (1979).

[8] J. C. Ashley and M. W. Williams, *Radiat. Res.* 81, 364-373 (1980).

[9] T. Inagaki, E. T. Arakawa, R. N. Hamm, and M. W. Williams, *Phys. Rev. B* 15, 3243-3253 (1977).

[10] C. J. Tung, J. C. Ashley, V. E. Anderson, and R. H. Ritchie, "Inverse Mean Free Path, Stopping Power, CSDA Range, and Straggling in Silicon and Silicon Dioxide for Electrons of Energy $\leq$10 keV," Air Force Report RADC-TR-76-125 (April 1976).

[11] E. J. McGuire, "Calculated Generalized Oscillator Strengths for the Atoms He-Na," Sandia Laboratories Report SC-RR-70-406 (May 1971).

[12] M. J. Berger and S. M. Seltzer, "Studies in Penetration of Charged Particles in Matter," National Academy of Sciences-National Research Council, Washington, D.C. (1964), Publ. No. 1133, pp. 205-268.

[13] L. Pages et al., *Atomic Data* 4, 1-127 (1972).

[14] W. Brandt, "Energy Loss and Range of Charged Particles in Compounds," E. I. du Pont de Nemours and Company Research Report (July 1960). NAPS Document No. 02194, to be ordered from ASIS-NAPS, c/o Microfiche Publications, 305 E. 46th Street, New York, N.Y., 10017. The stopping powers for electrons in these tables require a correction in the extrapolation procedure which leads to substantial increases in the low-energy stopping powers (J. C. Ashley and W. Brandt, to be published).

[15] C. J. Powell, *Rev. Mod. Phys.* 48, 33-47 (1976).

[16] J. C. Ashley (to be published).

Table I. Constants for Calculations of Mean Free Paths and Stopping Powers

Organic Material	Composition[a]				ρ[b]	M[c]	N[d]	n[au]×10^4)[e]	n_v[au]×10^2)[f]
	C	N	O	H					
Polyethylene	2			4	0.92	28.05	12	29.23	3.507
Polystyrene	8			8	1.05	104.1	40	8.985	3.594
Adenine	5	5		5	1.35	135.1	50	8.904	4.452
Guanine	5	5	1	5	1.58	151.1	56	9.317	5.218
Kapton	22	2	5	10	1.42	382.3	138	3.310	4.568
Anthracene	14			10	1.25	178.2	66	6.251	4.125
Bakelite	44		6	36	1.40	660.7	248	1.888	4.683
Makrolon	16		3	14	1.20	254.3	96	4.206	4.038
Plexiglas[g]	5		2	8	1.19	100.1	40	10.59	4.237
Mylar[h]	10		4	8	1.385	192.2	72	6.423	4.625
Cellophane	6		5	10	1.50	162.1	64	8.245	5.277
Rislan[i]	22	2	2	42	1.045	366.6	152	2.541	3.862
Nylon 6,6	12	2	2	22	1.13	226.3	92	4.450	4.094

[a] Composition of material in terms of the number of carbon (C), nitrogen (N), oxygen (O), and hydrogen (H) atoms per molecule or monomeric unit.

[b] Density of material in g/cm^3.

[c] Molecular weight in g/mol for the given composition.

[d] Number of valence electrons per molecule or monomeric unit.

[e] n[au] is the number of molecules or monomeric units per unit volume in atomic units (au); n[au] = 1.480×10^{-25} n[cm^{-3}].

[f] n_v[au] is the valence electron density in atomic units (au); n_v[au] = 1.480×10^{-25} n_v[cm^{-3}].

[g] Polymethyl methacrylate; same chemical composition as Lucite, Perspex, PMMA resist.

[h] Polyethylene terephthalate; same chemical composition as Melinex.

[i] Polyamide resin; same chemical composition as Nylon 11.

Table II. Contributions to Inverse Mean Free Paths and Stopping Powers Due to K-Shell Ionization in Carbon (C), Nitrogen (N), and Oxygen (O)

	$\sigma_K[\mathrm{au}]\times 10^3)^a$			$s_K[\mathrm{au}]\times 10^2)^b$		
E[eV]	C	N	O	C	N	O
300	0.131			0.142		
400	4.08			4.93		
600	9.66	3.59	0.163	13.5	5.95	0.331
800	12.1	5.69	1.83	18.9	10.2	4.03
1000	12.8	6.70	2.81	22.0	12.8	6.62
2000	11.0	6.77	3.93	23.1	15.7	11.3
4000	7.30	5.03	3.25	17.2	13.5	11.1
6000	5.44	3.92	2.64	12.8	11.3	9.54
8000	4.37	3.29	2.23	10.3	9.74	8.32
10000	3.68	2.78	1.94	8.67	8.49	7.39

[a] σ_K[au] is the ionization cross section per K shell in atomic units.

[b] s_K[au] is the stopping power due to K-shell ionization per K shell per unit volume in atomic units.

Table III. Stopping Powers (in eV/Å) of Some Organic Insulators

E(eV)	Kapton	Mylar	Bakelite	Plexiglas[a]
100	4.57	4.62	4.67	4.23
150	4.54	4.59	4.64	4.20
200	4.14	4.19	4.24	3.84
300	3.42	3.46	3.50	3.17
400	2.92	2.95	2.99	2.70
600	2.30	2.31	2.36	2.12
800	1.92	1.93	1.97	1.76
1,000	1.66	1.67	1.71	1.52
2,000	1.04	1.04	1.07	0.944
4,000	0.621	0.621	0.636	0.562
6,000	0.451	0.450	0.461	0.407
8,000	0.357	0.357	0.365	0.323
10,000	0.298	0.298	0.304	0.269

[a] Polymethyl methacrylate; also Lucite, Perspex, PMMA resist.

Table IV. Values of Parameters Required for Predictions of Stopping Power Per K Shell Per Unit Volume for Electrons with $E \leq 10$ keV from the Equation $s_K[au]E_K[au] = (a - b/U_K + c/U_K^2) \ln U_K / U_K^p$ for Carbon (C), Nitrogen (N), and Oxygen (O)

	C	N	O
a	16.4	8.77	10.1
b	38.1	11.4	15.9
c	26.6	4.63	7.98
p	1.15	0.950	1.00
E_K[au][a]	10.4	14.8	19.7
E_K[eV]	282	402	537
% Diff.[b]	≤4%	≤1%	≤2%

[a] $E_K[au] = E_K[eV]/27.2$.

[b] This is the percentage difference in the values predicted by the fit equation for $U_K \geq 1.5$, using parameters in this table, from those presented in Table II.

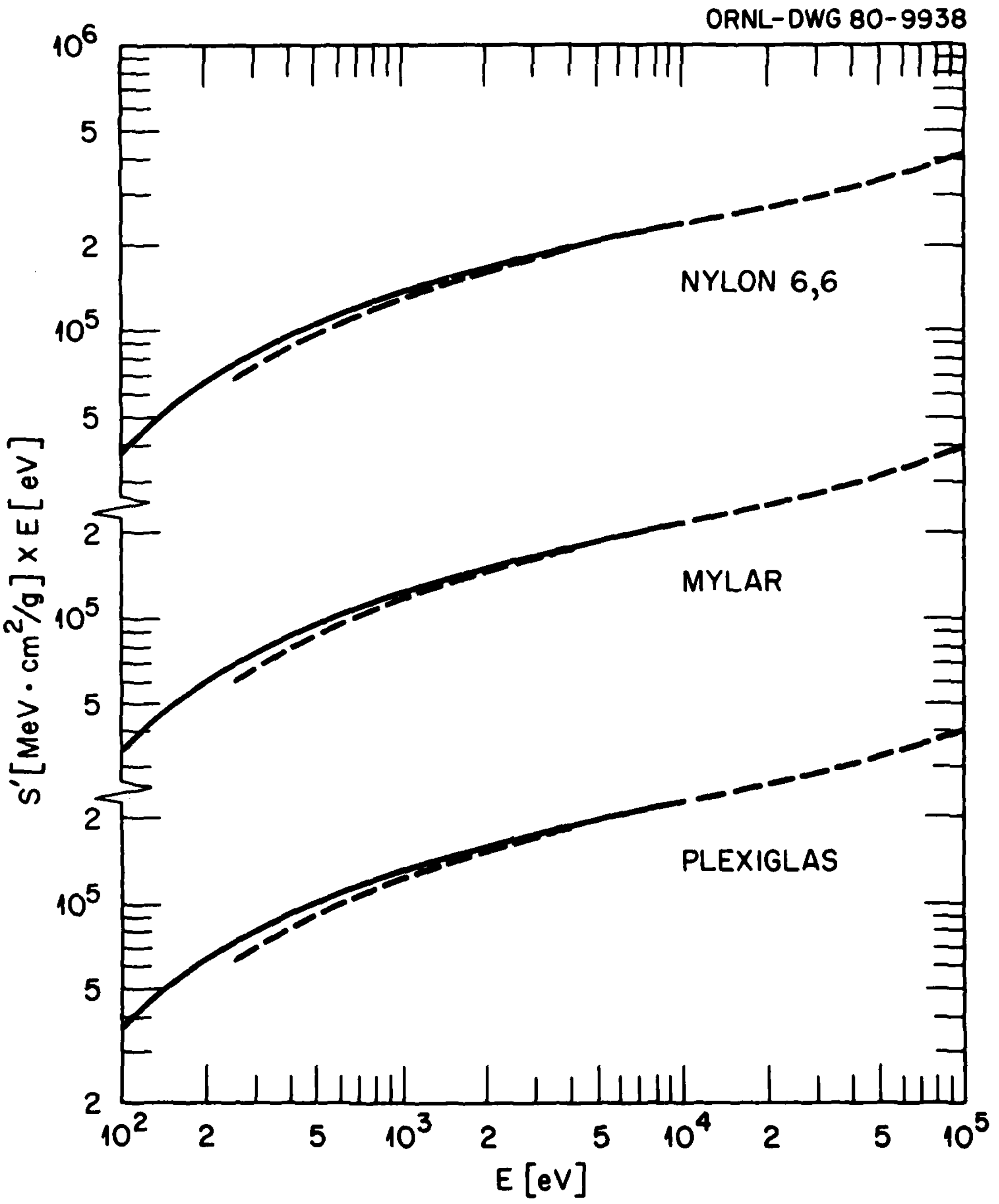

Fig. 1. Stopping powers, $S'=S/\rho$, as functions of electron energy for three solid organic insulators. Solid curves from this work; dashed curves from Ref. 14.

MISSION
of
Rome Air Development Center

RADC plans and executes research, development, test and selected acquisition programs in support of Command, Control Communications and Intelligence (C^3I) activities. Technical and engineering support within areas of technical competence is provided to ESD Program Offices (POs) and other ESD elements. The principal technical mission areas are communications, electromagnetic guidance and control, surveillance of ground and aerospace objects, intelligence data collection and handling, information system technology, ionospheric propagation, solid state sciences, microwave physics and electronic reliability, maintainability and compatibility.

Printed by
United States Air Force
Hanscom AFB, Mass. 01731